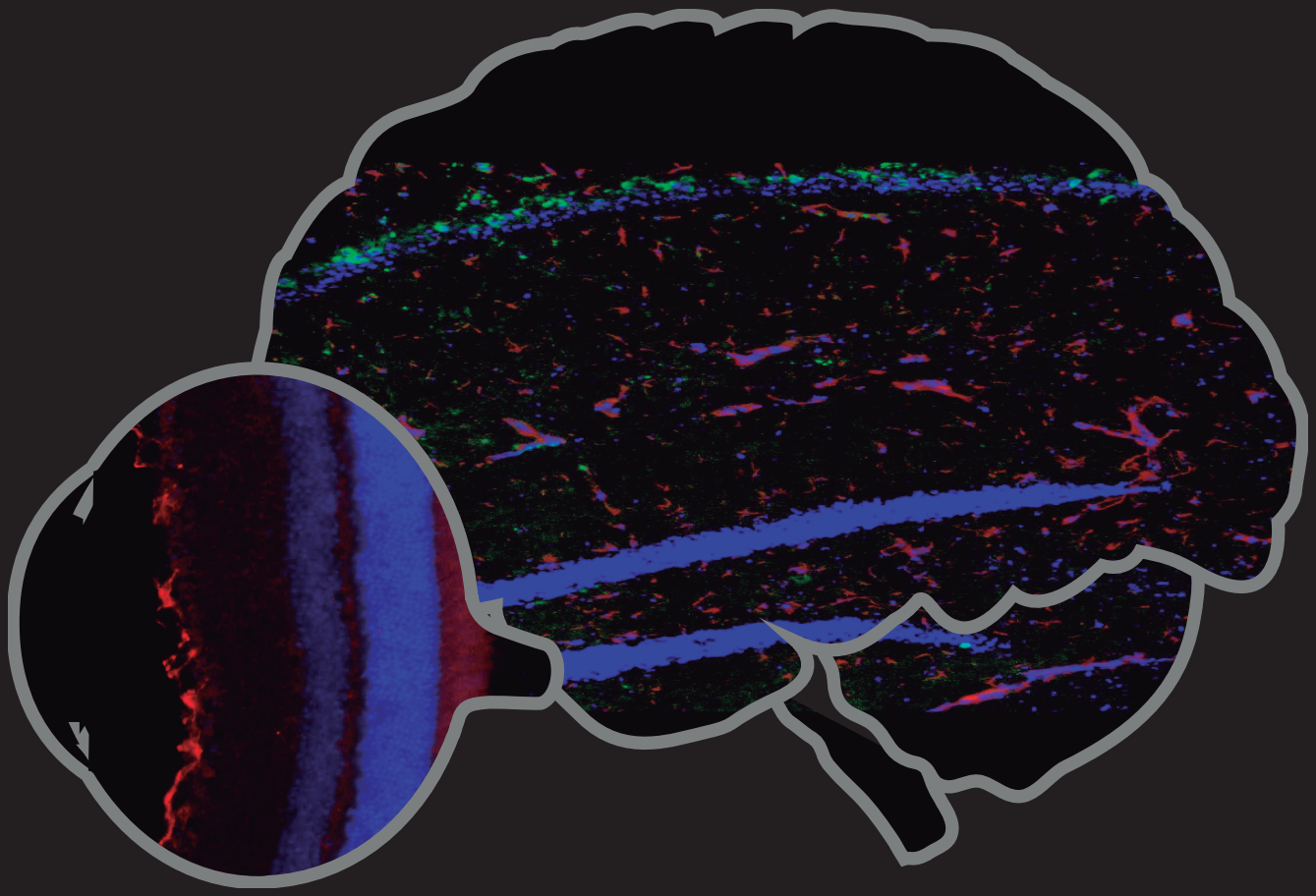

Rafael José Monteiro Carecho

CAN THE RETINA BE A WINDOW TO THE CHANGING BRAIN IN ALZEIMER'S DISEASE?

Dissertação de Mestrado em Investigação Biomédica, sob a orientação do Doutor António Francisco Rosa Gomes Ambrósio e da Doutora Filipa Isabel Cabaço Baptista e apresentada à Faculdade de Medicina da Universidade de Coimbra

Julho 2017

· U C ·

Universidade de Coimbra

On the front page: Hippocampus and retina of 3xTg-AD mice stained with GFAP (red) and Aβ (6E10) (green). Nuclei stained with DAPI (blue).

CAN THE RETINA BE A WINDOW TO THE CHANGING BRAIN IN ALZHEIMER´S DISEASE?

Rafael José Monteiro Carecho

Dissertation presented to the Faculty of Medicine of the University of Coimbra to fulfill the necessary requirements to obtain the Master degree in Biomedical Research. The work was performed at the *Retinal Dysfunction and Neuroinflammation Lab* from the Institute of Biomedical Imaging and Life Sciences (IBILI), Faculty of Medicine, University of Coimbra, under the scientific supervision of Doctor António Francisco Rosa Gomes Ambrósio and co-supervision of Doctor Filipa Isabel Cabaço Baptista.

2017

The experimental work described in the present thesis was performed at *Retinal Dysfunction and Neuroinflammation Lab* at the Institute for Biomedical Imaging and Life Sciences (IBILI), Faculty of Medicine, University of Coimbra.

Financial support was granted by Santa Casa Mantero Belard Award 2015 (MB-1049-2015), Foundation for Science and Technology (PEst UID/NEU/04539/2013), COMPETE-FEDER (POCI-01-0145-FEDER-007440), and Centro 2020 Regional Operational Programme (CENTRO-01-0145-FEDER-000008: BRAINHEALTH 2020), (CENTRO-01-0145-FEDER-000012: HEALTHYAGING 2020).

Agradecimentos

Esta secção é para mim especial, pois durante toda a minha vida aprendi o valor da gratidão, da importância de sabermos sentir-nos agradecidos pelo que temos e pelo tanto que nos é dado gratuitamente. Por esse motivo, o agradecimento que dedico a estas pessoas é feito de coração cheio e com o sentimento de mais uma etapa cumprida.

Ao Francisco, meu orientador e líder de grupo começo por agradecer a confiança e a amizade que desde o início estiveram sempre presentes. Por sempre me ter feito sentir à vontade e de portas abertas para decidir em função de uma única premissa, ser feliz. Pela oportunidade de desenvolver este trabalho e pelo acolhimento no seu extraordinário grupo, obrigado.

À Fi, por todo o apoio, paciência e compreensão, pela fonte inesgotável de serenidade e calma necessárias para encarar os momentos menos bons, quando as coisas não correm como gostaríamos e pela capacidade de encontrar soluções para grande parte dos problemas, obrigado.

Ao Professor Henrique Girão, por coordenar um mestrado de excelência, por aliar tão bem o rigor e exigência científica à parte humana. Pelo incansável apoio a todos os seus alunos e a disponibilidade demonstrada mesmo quando parece ser-lhe impossível, obrigado.

Um obrigado muito especial à Catarina Neves, por ter sido uma exemplar colega de trabalho, por todos os ensinamentos e momentos de boa disposição diários, pela capacidade de improvisar, de pensar, de agir e de se organizar mesmo no meio da minha desorganização, obrigado.

Ao Fábio e à Carla, pelas tantas conversas e desabafos entre horas de trabalho. Pelos cafés e jantares arranjados à última da hora quando a noite chegava sem avisar. Pela amizade de ambos, pelas ajudas, sugestões e partilhas de nada e de tudo, obrigado.

À Boia, à Rita e à Joana, por todos os momentos de descontração, pela companhia e por fazerem sempre do laboratório um lugar agradável onde reinam a boa disposição e

a entreajuda. Pela amizade, pelo apoio incansável e pela disponibilidade em todas as horas durante este ano, obrigado.

A todos os restantes colegas de grupo, Samuel, João, Elisa, Maria, Inês Almeida, Miguel, Inês Aires, Raquel Santiago, e a todos aqueles que durante este ano foram passando no laboratório, obrigado.

Aos meus amigos, em especial ao Marcelo, Marques, Ramos e Cláudio, pelos jogos de ténis, pelos disparates, pelos convites, pelos cafés, pelas cervejas, mas sobretudo pelos gestos reveladores de uma grande amizade, obrigado.

À Madalena por ser a uma das pessoas mais importantes de minha vida, pelo seu amor e apoio incondicional, por fazer de mim todos os dias uma pessoa melhor e me fazer sentir mais feliz a cada dia que passa. Por nunca duvidar do meu valor e de me mostrar sempre que sou capaz de fazer mais e melhor, obrigado.

Ao meu irmão, André, pela amizade e pela ajuda não só durante este ano, mas por estar sempre presente, obrigado.

Aos meus pais, as pessoas mais especiais da minha vida, pelo seu amor e carinho, pela compreensão demonstrada em todos os momentos, e por porem sempre o meu bem-estar à frente do deles. Por acreditarem sempre em mim, por me encorajarem a fazer tudo a que me proponho e por terem feito sempre tudo o que estava ao seu alcance para que nunca me faltasse nada. E não faltou. Quaisquer palavras nunca serão suficientes para lhes agradecer a minha vida. De qualquer forma, **muito obrigado!**

Este trabalho é por isso dedicado a todas estas pessoas que direta ou indiretamente contribuíram para a sua realização e por força das suas ações foram a minha verdadeira fonte de inspiração.

OBRIGADO

Part of the work developed in this thesis was presented in different national and international scientific meetings, as listed below:

António Francisco Ambrósio, Samuel Chiquita, Catarina Neves, **Rafael Carecho**, Filipa Baptista, Elisa Campos, Paula Moreira. **Can the retina be used as a reliable mirror to evaluate changes occurring in the Alzheimer's brain?** *Annual Meeting of the Association for Research in Vision and Ophthalmology.* Poster presentation. 7-11 May 2017.

Rafael Carecho, Catarina Neves, Filipa Baptista, Paula Moreira, António Francisco Ambrósio. **Are the main features of Alzheimer's brain mirrored by the retina?** *XV Annual Meeting of the Portuguese Society for Neuroscience.* Poster presentation. 25-26 May 2017.

Catarina Neves, Samuel Chiquita, **Rafael Carecho**, Filipa Baptista, Paula Moreira, A. Francisco Ambrósio. **The retina as a mirror of the alterations observed in Alzheimer's disease brain? Evaluation of structural, cellular and molecular changes.** *XV Annual Meeting of the Portuguese Society for Neuroscience.* Poster presentation. 25-26 May 2017.

Table of Contents

Abstract

Alzheimer's disease (AD) became the most common neurodegenerative disorder worldwide, as a consequence of a growing elderly population. AD is a multifactorial disorder characterized by the accumulation of amyloid-beta (Aβ) plaques followed by neurofibrillary tangles of hyperphosphorylated tau protein leading to a massive neuronal loss and brain homeostasis disruption. These alterations result in severe cognitive impairments and memory loss having a huge impact in AD patient's life. So far, AD does not have a cure or efficient treatments, possibly because they are applied at too advanced stages when neuronal loss is irreversible. Thus, there is an urgent need to drive forward improvements in healthcare and early diagnosis in order to change the current framework.

Recently, the retina, which is an extension of the brain, became an interesting research tool to investigate brain diseases since it is also affected during the AD course. When compared with brain, the retina has the advantage of being less complex structurally and easily more accessible to non-invasive exploration. Although there are several imaging techniques able to assess retinal alterations, many questions remain to be solved before using the retina as an instrument to diagnose early neurodegenerative alterations in the brain.

In the present study, our main objective was to clarify whether the retina can in fact mirror AD brain pathology, focusing on the early molecular and cellular changes occurring in both retina and brain. This would be essential to use the retina as a reliable window/mirror of the brain pathology for the early diagnosis of AD.

Based on several changes described on AD brain pathology, we assessed a large set of biological parameters in hippocampus, cortex and retina from 3xTg-AD animal model and age-matched wild-type animals (C57BL6/129S) in two early timepoints (4 and 8 months).

The assessment of key molecular players involved in AD pathophysiology revealed an early accumulation of Aβ peptides in hippocampus and cortex, but not in the retina, whereas phosphorylated tau protein levels increased in the three regions analyzed. The amyloid precursor protein levels and β-secretase enzyme levels and activity remain unchanged, which suggest that the accumulation of Aβ peptides is due to Aβ clearance deficits at these early timepoints. The synaptic dysfunction and

neuronal loss observed in AD pathology was not observed in 3xTg-AD mice at 4 and 8 months of age by evaluating synaptic protein levels and apoptotic cell death, respectively. Changes observed in GFAP protein levels in the hippocampus and retina suggest an increase of astroglial plasticity, whereas no differences in the number and distribution of microglia and Müller cells were noted. The increase of GFAP levels in the hippocampus at 4 months correlates with increased Aβ levels at this timepoint. The posterior analysis of mitochondrial metabolism suggests that there is an attempt to maintain a healthy mitochondrial pool and to restore the energy demands in hippocampus and cortex at 8 months, whereas in the retina no similar changes were observed.

Taken together, this group of results does not support the hypothesis that the retinal pathology mirrors brain alterations in the 3xTg-AD animal model, at least at the early timepoints analyzed. The assessment of later timepoints is necessary to draw more consistent conclusions.

Resumo

Como consequência do envelhecimento populacional, a doença de Alzheimer (DA) tornou-se a doença neurodegenerativa mais frequente em todo o mundo. A DA é uma doença multifatorial caracterizada pela acumulação de placas de β-amilóide (Aβ) e de tranças neurofibrilares constituídas maioritariamente pela proteína tau hiperfosforilada, as quais levam a uma perda neuronal massiva e consequente perda da homeostasia neuronal. Estas alterações resultam em défices cognitivos graves comprometendo, na grande maioria das vezes, a memória dos pacientes. Os tratamentos existentes disponíveis para a DA não são eficazes, possivelmente porque são administrados em fases demasiado avançadas da doença, quando a perda neuronal é irreversível. Assim, existe uma necessidade urgente de melhorar os tratamentos disponíveis e o diagnóstico precoce da doença.

A retina, tal como o cérebro, faz parte do sistema nervoso central, e recentemente tornou-se uma ferramenta interessante para investigar doenças cerebrais, uma vez que também é afetada em pessoas com doenças degenerativas do cérebro. A retina tem algumas vantagens relativamente ao cérebro. É uma estrutura menos complexa e mais acessível. Embora existam várias técnicas de imagem capazes de avaliar as alterações na retina, muitas questões ainda necessitam de ser esclarecidas antes de se poder utilizar a retina como uma ferramenta para diagnosticar precocemente alterações neurodegenerativas no cérebro.

No presente estudo, o principal objetivo consistiu em esclarecer se a retina pode, de facto, espelhar a patologia do cérebro na DA, tendo como foco uma avaliação, em paralelo, das alterações moleculares e celulares precoces que ocorrem na retina e no cérebro. A clarificação desta questão será essencial para utilizar a retina como uma janela/espelho que permita avaliar com confiança a patologia do cérebro de modo a permitir um melhor diagnóstico precoce da AD.

Tendo como base as várias alterações celulares e moleculares cerebrais descritas na DA, avaliou-se um conjunto de parâmetros biológicos no hipocampo, córtex e retina de um modelo animal de DA (3xTg-AD) e de animais controlo (C57BL6/129S), em dois estadios precoces da doença (4 e 8 meses de idade).

A avaliação dos principais marcadores moleculares envolvidos na fisiopatologia da DA revelou uma acumulação precoce de péptidos Aβ no hipocampo e no córtex, mas

não na retina. Os níveis de proteína tau fosforilada aumentaram nas três regiões analisadas. Os níveis de proteína precursora amilóide, bem como os níveis e atividade da enzima β-secretase permaneceram inalterados, sugerindo que a acumulação de péptidos Aβ será devida a défices na remoção de Aβ nestes estadios iniciais.

Não se detetou disfunção sináptica e perda neuronal, características da DA, nos murganhos 3xTg-AD, aos 4 e 8 meses de idade. As alterações observadas nos níveis de proteína GFAP no hipocampo e na retina sugerem um aumento da plasticidade astroglial. O aumento dos níveis de GFAP no hipocampo aos 4 meses ocorreram paralelamente ao aumento dos níveis de Aβ. Não foram detetadas alterações nas células da microglia e nas células de Müller.

A análise do metabolismo mitocondrial sugere que haverá uma tentativa de manter uma população mitocondrial saudável e de restaurar as necessidades energéticas no hipocampo e no córtex, aos 8 meses, enquanto que paralelamente, na retina, não se registaram alterações.

Os resultados obtidos não suportam a hipótese de que a retina reflete alterações cerebrais presentes no modelo animal 3xTg-AD, pelo menos nas fases precoces da doença. É necessário proceder à avaliação de estadios posteriores para se poderem tirar conclusões mais consistentes.

List of illustrations

List of tables

List of abbreviations and acronyms:

#
3xTg-AD | triple transgenic animal model of AD
A

ACh | Acetylcholine
AD | Alzheimer's Disease
AP | Alkaline phosphatase
APH-1 | Anterior pharynx defective 1
APOE | Apolipoprotein E
APP | Amyloid precursor protein
ATP | Adenosine triphosphate
Aβ | Amyloid-beta
B

BACE | β-site APP cleaving enzyme
BCA | Bicinchoninic acid
BRB | Blood-retinal barrier
BSA | Bovine serum albumin
C

CA | *Cornu Ammonis*
CAPS | N-cyclohexyl-3-aminopropanesulfonic acid
ChAT | Choline acetyltransferase
CNS | Central nervous System
COX | Cytochrome c oxidase
CSF | Cerebrospinal fluid
cyt c_{red} | Reduced cytochrome c
D

DAPI | 4',6'-diamidino-2-phenylindole
DCPIP | 2,6-dichlorophenolindophenol
DTT | Dithiotreitol
E

ECF | Enhanced chemifluorescent
ECL | Enhanced chemiluminescence
ELISA | Enzyme-Linked Immunosorbent Assay
ERG | electroretinogram
F

FAD | Familial AD
G

GCL | Ganglion cell layer
GFAP | Glial fibrillary acid protein
H

HEPES | 2-[4-(2-hydroxyethyl)piperazin-1-yl]ethanesulfonic acid
HRP | Horseradish peroxidase
I

IHC | Immunohistochemistry
INL | Inner nuclear layer
IPL | Inner plexiform layer
L

LTP | Long Term Potentiation
M

MAP | Microtubule-associated proteins
MHC | Major histocompatibility complex
MRI | Magnetic resonance imaging
N

NFL | Nerve fiber layer
NFT | Neurofibrillary tangles
NMDA | N-methyl-D-aspartate
O

OCT | Optimal Cutting Temperature
ONL | Outer nuclear layer
OPL | Outer plexiform layer
OXPHOS | Oxidative phosphorylation
P

PBS | Phosphate-buffered saline
PEN-2 | Presenilin Enhancer 2
PFA | Paraformaldehyde
PHF | Paired helicoidal filaments
PiB-PET | Pittsburg Compound B - positron emission tomography
PMSF | Phenylmethanesulfonyl fluoride
PS-1 | Presenilin 1
PS-2 | Presenilin 2
p-tau | phosphorylated tau
R

RFU | Relative fluorescence units
RGCs | Retinal ganglion cells
ROS | Reactive oxygen species
RPE | Retinal pigment epithelium
RT | Room temperature
S

SAD | Sporadic AD
SDS-PAGE | Sodium dodecyl sulfate-polyacrylamide gel electrophoresis
SEM | Standard error of the mean
T

TBS-T | Tris-buffered saline Tween-20
TUNEL | Terminal deoxynucleotidyl transferase (TdT)-mediated dUTP nick end labeling List of abbreviations and acronym
W

WB | Western blotting
WT | Wild-type

Introduction

1. Introduction

1.1. Overview of Alzheimer's Disease

In 1906, a German psychiatrist and neurologist described for the first time a neurological condition that became known by his name, Alzheimer's disease (AD). The disorder was firstly observed in a 51-year-old-female Alzheimer's patient known as Auguste Deter who had suffered from memory and comprehension deficits. When she died, Alzheimer reported, after postmortem examination in 1907, several pathological conditions such as shrinkage of the cortex, severely enlarged ventricles, the presence of unusual deposits and neurofibrillary tangles, which today are recognized as features of AD (Alzheimer 1907; Stelzmann et al. 1995; Small & Cappai 2006).

More than one hundred years later, despite all efforts around AD and other neurodegenerative disorders research and the great progress in our understanding of these pathologies, the number of people with dementia reaches almost 47 million worldwide and this figure is projected to double every 20 years reaching about 131.5 million cases in 2050 as consequence of population aging. According to the data presented in the World Alzheimer Report 2015 which analyzed the global impact of dementia, the total estimated cost was more than 700 billion euros, a huge economic impact worldwide (Alzheimer's Disease International (AZ) 2015 report). Nevertheless, the care provided is too often uncoordinated and disconnected, which is not able enough to provide the best care and respond to the people needs. Thus, there is an urgent need to drive forward improvements in healthcare and early diagnosis in order to change the current framework.

1.1.1. Clinical manifestations of AD

The growing elderly population became a current reality and with it arose the problems related with neurodegenerative disorders. AD is a form of dementia very common especially among elderly people, affecting a large percentage of individuals with more than 65 years old (Alzheimer's Disease International (AZ) 2015 report). However, it is important to differentiate the normal aging and dementia state. Dementia

results from a significant neuronal deterioration which provokes the loss of cognitive abilities severe enough to interfere with daily life activities, which is not a feature of a normal aging (Scheltens *et al*, 2016).

The average time course of illness is about 10 years until the disease inevitably culminates in death, but the clinical phase is preceded by pre-clinical (or pre-symptomatic) stage, which may last for two decades, during which the cognitive abilities start being affected. The symptoms can diverge in severity and chronology, but they mirror the gradual progression of degenerative changes that occur in the brain. Three clinical phases of AD may be defined according to progression and severity of disease, which are considered as mild (prodromal), moderate and severe AD (Holtzman et al. 2011; Masters et al. 2015). The disease begins when the pyramidal neurons in the entorhinal cortex are affected, leading to impairments in episodic memory which is related to personally experienced events (White & Ruske, 2002; Palmer, 2011). As the disease progresses, deficits in neurons are spread to other brain regions, particularly the hippocampus and neocortex. The extension of these cognitive impairments leads to disturbances in semantic memory (facts and general knowledge), language, attention, spatial orientation and executive functions, frequently accompanied by behavioral and psychological symptoms of depression and anxiety, becoming even harder the ability of AD patients to operate independently of their caregivers, whereas the memory responsible for habits and general skills remains preserved until the late stages of AD (Braak & Braak, 1991, 1998; Holtzman *et al*, 2011; Palmer, 2011).

Looking at this global framework something needs to be changed. The active and healthy aging must be more and more a global concerning and a real societal challenge for the next few decades. In parallel, novel therapeutic approaches, treatments and early diagnosis criteria are needed to improve the resources against neurodegenerative diseases in order to improve the life quality of elderly people as much as possible.

1.1.2. AD pathophysiology

AD is a multifactorial neurodegenerative disorder that present a complex pathophysiology. Senile plaques and neurofibrillary tangles are known as the main pathological hallmarks of AD and are respectively related to the extracellular

accumulation of amyloid-β peptide (Aβ) aggregates, and intracellular assembly of the hyperphosphorylated microtubule-associated tau protein in neurofibrillary tangles (NFT) (Figure 1), which promote several cytoskeletal changes that impair the axonal transport, neuronal structure and neuronal plasticity (Iqbal *et al*, 2005; Ittner & Götz, 2011; Scheltens *et al*, 2016). Aβ formation seems to be responsible to trigger hyperphosphorylation of tau (p-tau), however both proteins are able to amplify each other's toxic effects (Rhein *et al*, 2009b).

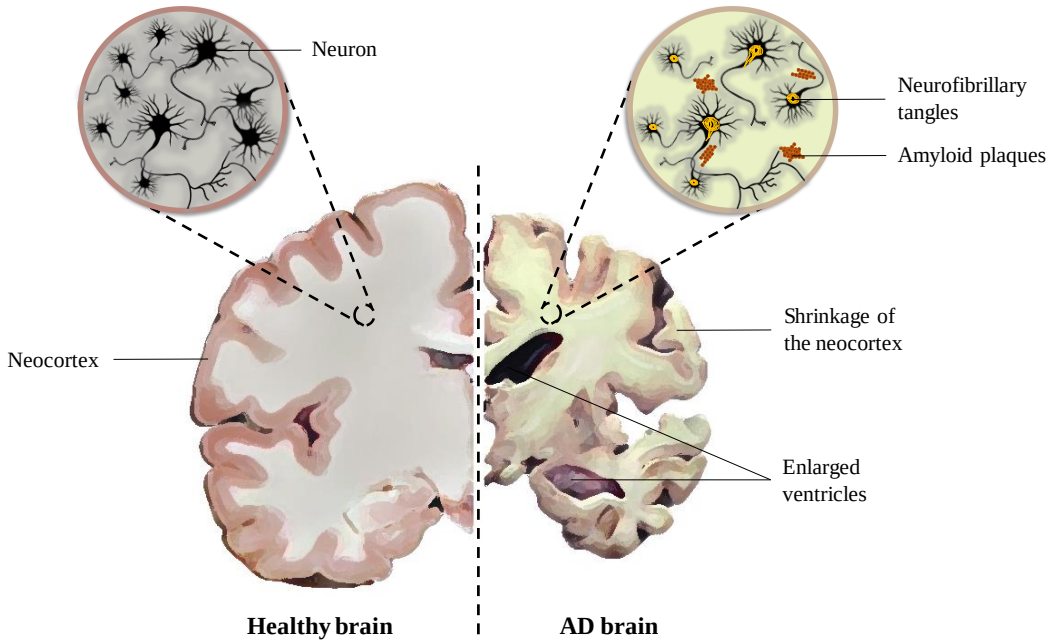

Figure 1 | Schematic representation of healthy and AD brain showing the main differences between healthy and pathological brain.

1.1.2.1. Amyloid-β pathology

Back in 1984, the researchers George Glenner and Caine Wong isolated and characterized for the first time "a novel cerebrovascular amyloid protein", now known as amyloid-β (Glenner & Wong, 1984). Closely associated with AD, Aβ is considered one of the most important pathological features of this type of dementia, being the main component of the senile plaques found in the Alzheimer patients' brain (Selkoe & Hardy, 2016). It is the product of amyloid precursor protein (APP) processing, which is a transmembrane protein with a large extracellular domain which can be found not only in the cell surface but also in plasma membrane of several organelles such as

endoplasmic reticulum and mitochondria. There are about 10 APP isoforms generated by alternative splicing that are ubiquitously expressed in human tissues being that the most common isoform in central nervous system (CNS), the one that results in 695 amino acids (Kang *et al*, 1987; O'Brien & Wong, 2011).

APP can be processed by two distinct antagonist pathways. In the non-amyloidogenic pathway, which does not generate Aβ, APP is metabolized directly by α- and γ-secretase, releasing different fragments, including its extracellular domain (sAPPα), which is known to have neurotrophic effects (Chasseigneaux & Allinquant, 2012). Alternatively, Aβ results from the amyloidogenic pathway in which APP goes through sequential action of two different cleaving enzymes, firstly by β-secretase whose activity has been attributed to the aspartic protease β-site APP cleaving enzyme (BACE) and then by γ-secretase which is a multi-subunit protease complex composed by four components: presenilins (PS-1 and PS-2), nicastrin, anterior pharynx defective 1 (APH-1), and presenilin enhancer 2 (PEN-2) (Haass & Selkoe 1993; Chami & Checler 2012). From these cleavages, a smaller N-terminal fragment (sAPPβ) and the Aβ peptide are released, which may vary according to the number and sequence of amino acids, depending on the γ-secretase cleavage site (Figure 2).

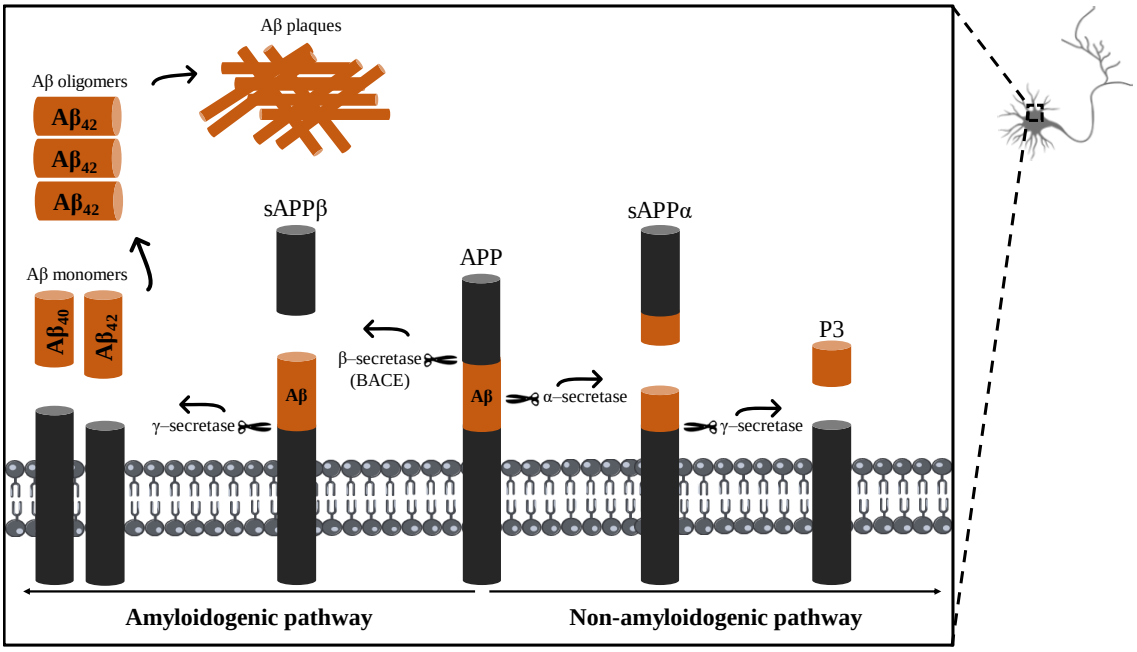

Figure 2 | Schematic representation of the two distinct pathways of APP processing and the main enzymatic players involved. The non-amyloidogenic pathway does not generate Aβ whereas the amyloidogenic pathway results in Aβ monomers that progressively aggregate until deposit as plaques.

Thus, several Aβ species may be generated with different lengths, being the 40 amino acid sequence ($A\beta_{40}$) the most abundant in the brain under normal conditions (Seubert *et al*, 1992). However, in AD patients, for several possible explanations, there is an increase in the Aβ long form with 42 amino acids ($A\beta_{42}$), which is the most neurotoxic amyloid species and has more prone to aggregation (Roher *et al*, 1993; Snyder *et al*, 1994). As they are produced, they are released into the extracellular space as monomers which progressively aggregate into dimers, oligomers, fibrils until generate the insoluble senile plaques (O'Brien & Wong 2011; De-Paula et al. 2012) (Figure 2).

The accumulation of these aggregates represents the beginning of several events that lead to neuronal homeostasis disruption (amyloidogenic cascade). They are the causative agents of neurotoxicity in AD and interact with neurons and glial cells promoting the activation of pro-inflammatory cascades, mitochondrial dysfunction, neuroplasticity decrease, deficits in calcium metabolism, impairment of intracellular signaling and synaptic function (impairs long-term potentiation), and increase in tau phosphorylation that finally lead to the induction of neuronal apoptosis (Selkoe, 1991). These events amplify Aβ-related neurotoxicity as a positive feedback loop exacerbating the pathological condition associated with amyloid plaques (Figure 3).

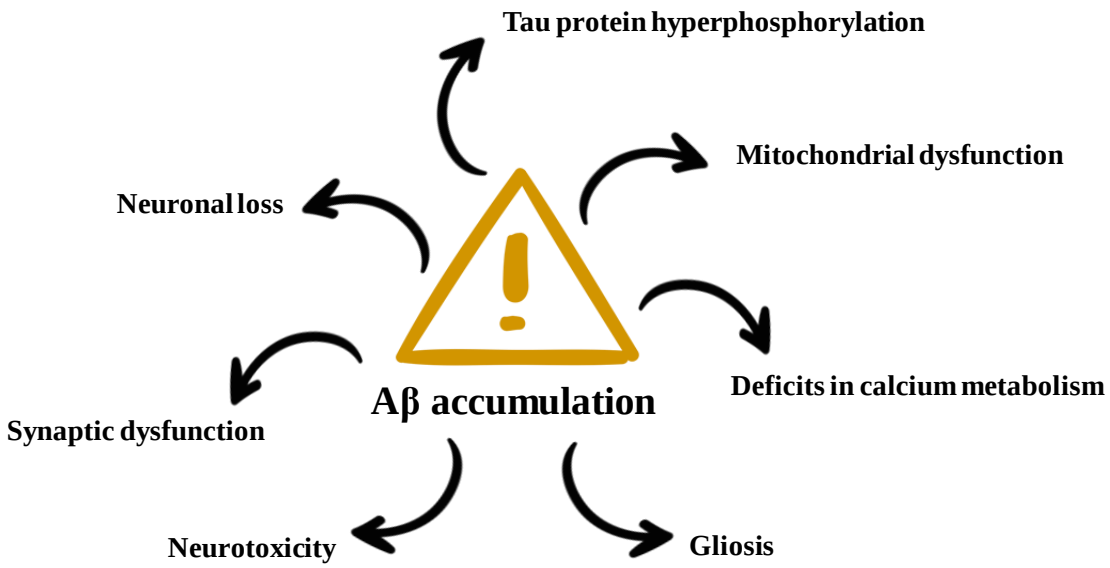

Figure 3 | Amyloidogenic cascade. The main subsequent events to Aβ accumulation.

Previous studies have shown that Aβ can spread intracellularly and trans-synaptically along neuronal connections (Takahashi, 2004; Nath *et al*, 2012), thereby expanding plaque pathology throughout the brain, starting in neocortex (Thal *et al*, 2002). Moreover, intraneuronal Aβ may serve as a source for the extracellular amyloid deposits (Oddo *et al*, 2006). Nevertheless, several studies defend that Aβ is not always associated with neurotoxicity, and may even be neuroprotective, particularly at low concentrations, which do not allow the oligomerization. (Whitson *et al*, 1989; Yankner *et al*, 1990; Chen & Dong, 2009; Chasseigneaux & Allinquant, 2012).

1.1.2.2. Tau pathology

Tau protein was identified for the first time in 1975 by Weingarten and colleagues in Marc Kirschner's laboratory at Princeton University. They described it as a critical protein for microtubule assembly. Tau protein belongs to the family of microtubule-associated proteins (MAP) by interacting with tubulin (Weingarten *et al*, 1975). Normally, tau is predominantly found in axons and plays a central role in the maintenance of neuronal structure as well as in the axonal transport of vesicles containing neurotransmitters (De-Paula et al. 2012). In the adult human brain, six tau isoforms resulting from a single gene mRNA alternative splicing have been described. These isoforms differ from each other in the number of tubulin-binding domains. They may still undergo post-translational modifications including glycosylation, oxidation and phosphorylation (Ittner & Götz, 2011).

The interaction of tau with tubulin is regulated by phosphorylation at multiple sites (there are about 84 currently known) by several kinases. When tau is abnormally phosphorylated, it loses the ability to bind to microtubules resulting in its detachment and consequently accumulation (Selden & Pollard, 1983; Pierre & Nunez, 1983; Lindwall & Cole, 1984). These events lead to the reassembly of tau into paired helicoidal filaments (PHF) which are the main component of NFT (Grundke-Iqbal *et al*, 1986; Brion *et al*, 1991). At this hyperphosphorylated state, the PHF-tau complexes may have until eight phosphate groups per molecule of tau, in opposition to the healthy brain where the usual degree of phosphorylation is two phosphate groups per molecule (De-Paula et al. 2012) (Figure 4).

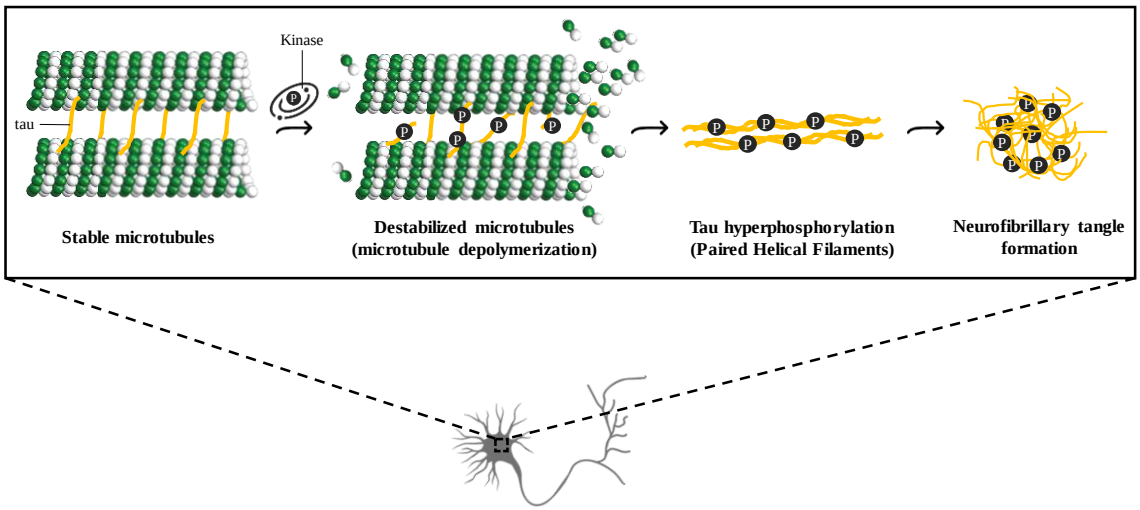

Figure 4 | Schematic representation of tau pathology. When tau is hyperphosphorylated, it dissociates from microtubules, causing their depolymerization. Tau is then deposited in aggregates forming the neurofibrillary tangles (NFTs).

Because of high neuronal plasticity observed during the embryonic stages of development, neuronal tau is predominantly in its hyperphosphorylated state (Goedert *et al*, 1993; Brion *et al*, 1993). On the other hand, in a mature and healthy brain, the neuronal homeostasis and cytoskeletal stability is maintained mainly by a dephosphorylated state, although dynamic changes in tau phosphorylation are needed for neuronal responses (Johnson & Stoothoff, 2004). However, under pathological conditions as observed in AD, when tau is abnormally hyperphosphorylated generate the NFT, impairing its ability to bind tubulin, leading to cytoskeleton collapse and consequently deficits in axonal transport and synaptic metabolism that ultimately cause the cell loss (Drechsel *et al*, 1992). Consistent with the clinical presentation, this sequence of events start in the entorhinal region and then spreads to the hippocampus, amygdala and finally neocortex (Braak & Braak, 1991).

1.1.3. Neuronal loss and synaptic dysfunction in AD

Triggered by main features of AD aforementioned, the number of neurons start decreasing and those that remain become less well connected to their synaptic partners

leading to disruption of neuronal network and brain atrophy as disease progresses (Serrano-Pozo *et al*, 2011). In the advanced stages, this neuronal loss results in enlarged ventricles and severe brain shrinkage that correlates with the severity of cognitive symptoms (Jack *et al*, 2010). Severely affected regions include hippocampus (particularly the CA1, CA3 and dentate gyrus subfields), entorhinal cortex, amygdala and neocortex, in which high densities of plaques and tangles have been found (Palmer, 2011; Padurariu *et al*, 2012). In fact, long-term exposure to Aβ induces neurotoxicity, especially the oligomeric forms of $A\beta_{42}$ (Pike *et al*, 1993). Although the mechanisms by which Aβ and tau protein induces neuronal death are not completely understood, they may involve alterations in intracellular calcium, production of inflammatory mediators, axonal transport disruption, synaptic loss as well as decreases in certain neurotransmitters (Kar *et al*, 2004).

Pyramidal neurons are particularly vulnerable in AD. They use excitatory amino acids as neurotransmitters, principally the L-glutamate and L-aspartate and play a critical role in memory function. Impairments in neuronal N-methyl-D-aspartate (NMDA) receptors have been correlated with deficits in memory and learning (Morris *et al*, 1986). Also, the cholinergic neurons, which are related with attention and memory processes and whose main neurotransmitter is acetylcholine (ACh) are usually affected in AD. Postmortem analyses in AD patients brain shown decreased enzyme activity of choline acetyltransferase (ChAT), which is responsible for the synthesis of ACh (White & Ruske, 2002). Other studies have also shown that antagonists of cholinergic receptors promote several impairments in cognition (Robbins & Murphy, 2006). From this data, several drugs were developed for the treatment of AD but they have just provided modest symptomatic benefit.

1.1.4. Neuroinflammation in AD

Up to a certain threshold, inflammation is an important defence mechanism against either internal or external insults. In the brain, neuroinflammation is mainly carried out by microglia and astrocytes, two types of glial cells, which seem to change during the course of disease.

Astrocytes are highly versatile cells being important in neurotransmission, neurogenesis and synaptogenesis. In response to a stimulus, they proliferate, change its morphology and increase the expression of glial fibrillary acid protein (GFAP) in a process known as astrogliosis (Sofroniew & Vinters, 2010; Verkhratsky *et al*, 2015).

Microglial cells, in turn, are known as the resident macrophages of CNS and are permanently in surveillance of their surrounding microenvironment by extending and retracting their highly motile processes to eliminate the presence of pathogens and cellular debris. When they become reactive, they change its morphology from a ramified form with long processes to an amoeboid form. Moreover, microglia also play a critical role in the maintenance of neuronal plasticity and contribute to the protection and remodelling of synapses (Kettenmann *et al*, 2011; Heneka *et al*, 2015).

When the brain become more susceptible as result of aging or neuropathological conditions, microglia show enhanced sensitivity to inflammatory stimuli in a process known as microglial priming (Heneka *et al*, 2015). Although unclear, it is likely that the chronic exposure to neuronal debris and Aβ may induce microglial priming leading to an exacerbated inflammatory response (Hoeijmakers *et al*, 2016). In fact, glial activation triggered by Aβ starts a rapidly inflammatory response characterized by release of pro-inflammatory mediators that may contribute to disease progression and severity (Patel *et al*, 2005). Both microglia and astrocytes are commonly associated to protein aggregates (Itagaki *et al*, 1989) being that microglia are able to surround plaques and internalise Aβ (Bolmont *et al*, 2008). These evidences suggest that in AD, Aβ is the main driver to neuroinflammation and that glial cells lose some of their homeostatic and neuroprotective capabilities (Verkhratsky *et al*, 2015) (Figure 5).

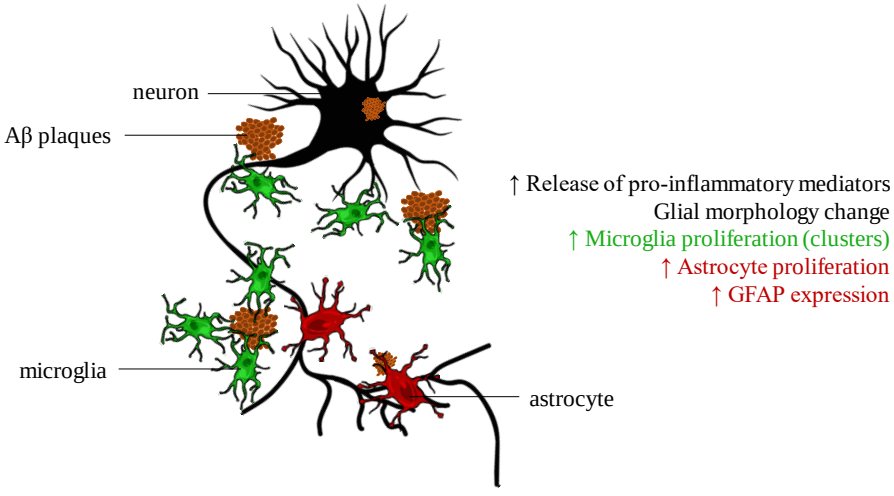

Figure 5 | Glial response to Aβ chronic exposure. Microglia and astrocytes become reactive, proliferate and release pro-inflammatory mediators increasing the neuroinflammatory environment.

1.1.5. Mitochondrial dysfunction

Mitochondria are key organelles in the majority of eukaryotic cells providing them energy through the ability to oxidize nutrients in oxidative phosphorylation (OXPHOS) pathway, thereby releasing energy used for adenosine triphosphate (ATP) generation. Given that neurons are cells with high energetic requirements, the mitochondrial proper functioning is obviously critical to sustain neuronal function and integrity (Carvalho *et al*, 2015a; Cardoso *et al*, 2016).

Therefore, it is acceptable that the dysfunction of mitochondrial network dynamics may be responsible for the development of neuronal injuries and enhanced apoptosis. In fact, in neuropathological conditions like AD, alterations at the level of mitochondrial respiratory enzyme complex activities drive to an overproduction of reactive oxygen species (ROS) and increase the oxidative stress that causes a general impairment all over the cell (Caspersen 2005).

There is evidence that Aβ peptides progressively accumulate within mitochondria where it can bind and inhibit Aβ-binding alcohol dehydrogenase and promote mitochondrial generation of free radicals (Lustbader, 2004). Aβ also interferes with mitochondrial NADH dehydrogenase (complex I) decreasing its activity and it also can bind to heme groups from cytochrome c oxidase (COX, complex IV) thereby reducing its activity and impairing the respiratory chain function contributing even more to increased ROS production and decreased ATP synthesis (Carvalho *et al*, 2013).

Furthermore, hyperphosphorylated tau protein may also affect the proper function of mitochondrial enzymatic proteins acting synergistically with Aβ accelerating the deficits found in respiratory capacity and particularly in COX activity (Rhein *et al*, 2009b).

Interestingly, there is also consistent data demonstrating several alterations in expression and activity of respiratory mitochondrial enzymes like isocitrate dehydrogenase, COX, pyruvate dehydrogenase, among others, before the appearance of both Aβ and p-tau proteins as well as the onset of memory deficits (Manczak *et al*, 2004; Yao *et al*, 2009; Chou *et al*, 2011).

Further investigation is needed in order to clarify what is cause or consequence of disease onset and progression.

1.1.6. Risk factors of AD

In the last few decades AD became one of the most investigated pathology. The scientific community has been spending a lot of time trying to identify several factors able to increase or decrease a person's chances for developing the disease. Aging is the most known and probably the most worrying factor, whose risk increases to double every 5 years after age 65. In addition, there are many others linked to an increased risk of developing AD that in a certain way can be changed or controlled by people and include diabetes, hypertension, obesity, regular smoking, high cholesterol, physical and mental inactivity, among others (Reitz & Mayeux, 2014; Imtiaz *et al*, 2014). Supporting these evidences, several studies have shown that regular physical exercise (Hamer & Chida, 2009) as well as a high cognitive stimulation have a preventive effect in AD (Lazarov et al. 2005).

Genetics also plays an important role in AD development. Several genes have been linked to an increased risk to develop the disease. Apolipoprotein E (*APOE*) was the first risk gene identified (Saunders et al. 1994) and today is still the one with higher impact. Currently, the risk factors aforementioned are those that have been associated with sporadic AD (SAD), which is the most common form of the disease. It accounts for more than 95% of all AD cases with late onset that usually is after age 65. On the other hand, there is also the familial AD (FAD) form which is inherited as an autosomal dominant disorder with mutations in the *APP*, *PSEN-1* and *PSEN-2* genes. However, it accounts for only 5% of all AD patients. Usually, its symptoms appear between 30 and 65 years, which means that FAD patients have an earlier onset and faster progression than SAD cases (Piaceri *et al*, 2013).

1.1.7. Genetic landscape of AD

Recently, one of the major focus in AD research has been to understand the genetic etiology and its relationship with AD neuropathology and the more we know, the more we realize that indeed genes play a critical role in its development. Regarding the genetic risk factors aforementioned, we can distinguish two types of genetic contributions.

On the one hand, related to SAD, *APOE* gene has been confirmed as a susceptibility risk factor. It is a polymorphic gene with three major alleles, *ε2*, *ε3* and *ε4*, mapped in the long arm of the chromosome 19. Thus, *APOE* is expressed in three possible genetic isoforms with 299 amino acids, ApoE2, ApoE3 and ApoE4 (Williamson *et al*, 2009). Several evidences show that people who inherit one or two *ε4* alleles have an even higher risk to develop AD (Farrer *et al*, 1997) whereas ApoE2 is associated to neuroprotection (Conejero-Goldberg *et al*, 2014). In fact, the three isoforms stimulate Aβ synthesis differently (Huang *et al*, 2017) and decrease Aβ clearance (Castellano *et al*, 2011), with an ApoE4 > ApoE3 > ApoE2 potency rank order. These variations are related with differences in 1 or 2 amino acids in the sequence between ApoE isoforms, which alter the total charge, protein structure and functional properties. Because of that, so different effects can be attributed to both ApoE4 and ApoE2 (Piaceri *et al*, 2013; Liu *et al*, 2013). Furthermore, many other genes have been identified and associated to an increased risk to develop SAD with late-onset (Giri M & Zhang M 2016).

On the other hand, as previously mentioned, FAD is linked to three mutations coding APP, PS-1 and PS-2 proteins. Usually it is diagnosed when more than one generation is affected by AD, but clinically it is similar to SAD (Piaceri *et al*, 2013). *APP* was the first mutant gene found on chromosome 21 related to the inherited form of AD (Goate *et al*, 1991), followed by mutations found in the genes encoding PS-1 on chromosome 14 (Sherrington *et al*, 1995) and PS-2 on chromosome 1 (Levy-Lahad *et al*, 1995), whose proteins make part of the catalytic core of γ-secretase complex. Mutations at the level of these three proteins enhance the production and deposition of $A\beta_{40}$ and $A\beta_{42}$. So far, over 200 different mutations that vary mainly in the location, have been described in these genes, being the mutations in *PSEN1* responsible for the majority of the cases of FAD (Ryan & Rossor, 2010).

Interestingly, the insights acquired from the study of mutations associated to FAD have catalyzed our understanding of disease, through the development of cellular and animal models harboring *APP*, *PSEN1* and *PSEN2* mutant genes.

1.1.8. Experimental models of AD

Transgenic models of AD are one of the most important research tools for understanding the underlying mechanisms and cause of disease in a manner that would be unethical or impractical in humans. In fact, the generation of transgenic mouse lines expressing genes associated with AD was an important step forward that made possible a huge development in AD research. However, although there are many genetic models for studying AD, it is important to highlight that neither of them display all features of the disease.

The first transgenic mouse models were created expressing human APP protein (e.g. Tg2576 and APP23), which only cause the development of Aβ pathology, but not NFT. The same happens with mice overexpressing the mutant isoform of PS-1 and PS-2. Regarding the double transgenic mice, APP/PS-1 and APP/PS-2, the accumulation and deposition of Aβ is faster than in single transgenic models and display behavioral and learning deficits. However, the late onset of pathological changes in the models mentioned above is responsible for some technical disadvantages. Therefore, in 2006 a new transgenic line was developed harboring five mutations, all responsible for the enhanced amyloid production, even faster than previous models. However, NFT is only detected when a mutation in tau protein is added, for example in the crossing of the Tg2576 mouse with a mouse expressing Tau_{P301L} (Bilkei-Gorzo, 2014).

In 2003, Oddo and colleagues developed a triple transgenic mouse model of AD (3xTg-AD) with C57BL6/129S genetic background. This transgenic animal model harbors three human mutant genes (APP_{swe}, $PSEN\text{-}1_{M146V}$ and Tau_{P301L}) that promote the development of an age-related and progressive neuropathological phenotype that includes both Aβ and tau pathology and resembles the neuropathological progression of human AD (Oddo *et al*, 2003). Nevertheless, the massive neuronal loss usually observed in AD pathology is strikingly absent from AD mouse models (Wirths & Bayer, 2010; Zahs & Ashe, 2010).

1.1.9. Diagnosis of AD

Currently, a definitive diagnosis of AD in the majority of cases can only be made after a postmortem examination revealing its cerebral hallmarks. Until there, whereas the patient is alive, diagnosis can only be designated as "probable". Recently, criteria proposed by International Working Group and National Institute of Aging and Alzheimer's Association recognized a pre-clinical stage (Scheltens *et al*, 2016) based on previous studies that show that changes start appearing in the brain several years before the first symptoms emerge (Bateman *et al*, 2012). This means that people who seem free of disease today may be at risk in a near future. There is no specific diagnosis for this stage, but the guidelines proposed a research agenda with the aim of identifying biomarkers that help to develop new diagnostic methods in order to signal the beginning of these pre-symptomatic changes, trying to stop AD progression. Furthermore, the recent failures of potential drugs for AD treatment may indicate that people in clinical trials are already in a disease advanced stage to drive a clinical benefit (Counts *et al*, 2017), reinforcing the need for an early detection.

Among several approaches, those with most promising results for a potential clinical application are the assays to quantify soluble Aβ monomers, tau and p-tau in the cerebrospinal fluid (CSF), whose $A\beta_{42}$ concentrations are found decreased whereas tau and p-tau are increased. Also, the advanced molecular imaging methods to detect amyloid burden in the brain with Pittsburg Compound B - positron emission tomography (PiB-PET) or even the assessment of mesial temporal lobe atrophy on magnetic resonance imaging (MRI) may eventually achieve an earlier and more specific diagnosis (De-Paula et al. 2012; Counts et al. 2017).

In fact, many efforts have been done to develop sophisticated and reliable tests to identify who is most likely to develop AD. However, they have not been sufficiently accurate and still present some practical limitations. Apart from being expensive and somewhat subjective, due to the lack of markers that help to distinguish AD from other dementias, these approaches are not widely available, precluding them from being used routinely in the clinic. Furthermore, the CSF sample collection is an invasive method and the PiB-PET imaging requires repeated exposure to radiation (Lim *et al*, 2016; Counts *et al*, 2017). Under this scenario, there is an urgent need of an early, accurate and definitive diagnosis of AD, with reliable and more readily accessible biomarkers

that mirrors the real features of disease in order to improve the weapons against disease progression.

In the last few years, based on evidences suggesting that one of the first complaints of AD patients refers to vision problems and that these visual deficits might be present before cognitive impairment or memory loss, the eye became an interesting tool for the study of the earliest pathophysiological changes involved in neurodegeneration, as well as for the development of new and more promising therapeutic approaches (Chang *et al*, 2014).

1.2. Retina

The visual system, where the eye is the main sensory organ, is responsible to receive light and convert it into electrochemical signals to the brain where information is processed allowing us to see the world. The eye is a very organized and functional structure being divided in three main layers: the sclera, the choroid and the retina which is comprised of several neuronal cell layers.

In fact, eye and brain establish a close relationship and share many similarities allowing that much of what is known from eye research could be relevant to the brain and vice versa. The retina, as well as, the optic nerve, extends from the neural tube sharing the same embryological origin as the brain. Because of that, the retina is considered an extension of the CNS exhibiting typical properties of brain and spinal cord including cell types, functionality and immunology (London *et al*, 2012). The retina is located inside the back of the eye and it is composed of three cell layers separated by two additional layers almost devoid of cell nuclei. In the outermost part, just before the choroid, there is a monolayer formed by cuboid pigmented epithelial cells called the retinal pigment epithelium (RPE). Adjacent to RPE is the outer nuclear layer (ONL), then the inner nuclear layer (INL) and, in the innermost part of the retina, the ganglion cell layer (GCL) that contains the retinal ganglion cells (RGCs) whose axons form the optic nerve (nerve fiber layer – NFL). On the ONL there can be found photoreceptors (rods and cones) that capture the light when it enters in the eye initiating a cascade of neuronal signals that then reaches the GCL. The INL features the horizontal, bipolar and amacrine cell nuclei. Before the GCL there is the inner

plexiform layer (IPL) where RGCs synapse with interneurons from INL, and before the INL there is the outer plexiform layer (OPL) (Hart *et al*, 2016) (Figure 6).

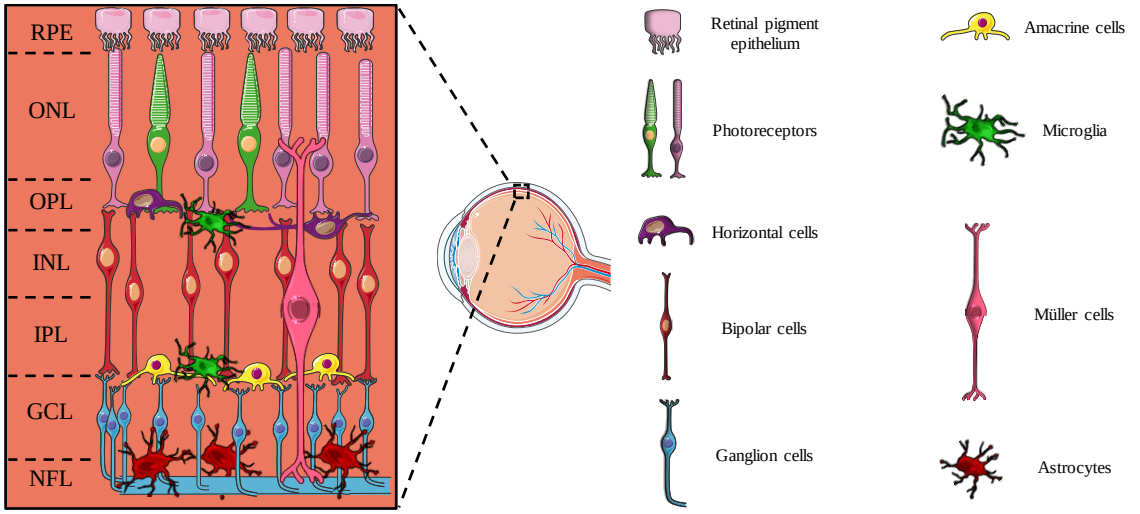

Figure 6 | Schematic representation of the major retinal cell layers. Photoreceptors, bipolar and ganglion cells provide the direct signaling pathway for visual information reach the brain. Horizontal and amacrine cells regulate interneural communication. Microglia, astrocytes and Müller cells contribute for retinal homeostasis maintenance (Adapted from Madeira et al. 2015) .

In addition to neurons, retina is also composed by glial cells which offer both structural and metabolic support as well as immune surveillance. In fact, as well as the brain, retina is also an immune-privileged site where glial cells provide specialized immune responses similar to those observed in the brain (Streilein, 2003). Three distinct types of glia can be found in the retina: Müller cells, astrocytes and microglia. Müller cells go across the entire thickness of the retina mediating homeostatic and metabolic mechanisms that support retinal neurons and also regulate synaptic activity. Astrocytes on the other hand are confined to the region formed by axons of RGCs. Their processes wrap around blood vessels having an important structural supportive role in the retina, and as well as the Müller cells, both integrate the vascular and neuronal activity in the retina. Microglial cells, the resident immune cells of the CNS, are essential for homeostatic regulation of the retina. They are mainly found on the IPL and GCL and have been implicated in neurogenesis, neuronal physiology and survival. As a result from chronic microglial activation, a dangerous increase of inflammatory mediators will

contribute to an even higher retinal degeneration observed in AD pathology (Kolb, 2001).

1.2.1. Retinal changes in AD

Given that many AD patients report visual deficits, there has been an increased interest in potential ocular biomarkers, particularly at the retinal level. In fact, studies previously performed have reported ocular changes in several neurodegenerative disorders opening doors to the eye as a research and diagnostic tool. Although some ocular manifestations are similar between diseases, their existence shows a strong crosstalk between the retina and the brain (London *et al*, 2012).

Over the last three decades, studies (reviewed in Lim et al. 2016) have shown that all parts of the visual system, including the retina and optic nerve, might be affected in AD. However, there are still controversial issues. Many studies using different models at different timepoints report different results, as reviewed in Shah et al. 2017.

The first histological evidence showing retinal abnormalities in AD was reported in 1986 by Hinton and colleagues, who described ganglion cell losses, a decrease of their axons and optic nerve degeneration (Hinton *et al*, 1986). These findings were corroborated by further studies (Lu *et al*, 2010; Cheung CY, Ong YT, Hilal S, Ikram MK, Low S, Ong YL, Venketasubramanian N, Yap P, Seow D, Chen CL, 2015) and suggest that NFL thinning is an early event in AD pathology (Paquet *et al*, 2007). However, in other studies, no changes in NFL thickness and no optic nerve degeneration were detected (Kergoat *et al*, 2001).

Curiously, regarding the pathological accumulation of Aβ in the retina there are also inconsistent studies, remaining unclear whether retinal amyloid plaques precede or not the plaques in the brain. Koronyo-Hamaoui and colleagues reported retinal Aβ plaques in postmortem eyes from AD patients (Koronyo-Hamaoui *et al*, 2011), whereas in other studies no changes were detected (Ho et al. 2014).

From electroretinogram (ERG) recordings, which give insight into the electrical response of the retinal neurons, while some groups have described a significant reduction in a- and b- waves in AD patients at the advanced stages as well as an

increased latency of the response (Parisi *et al*, 2001), others have not found abnormalities in synaptic dysfunction (Justino *et al*, 2001).

Regarding animal models of AD, there is a limited number of studies, mainly using the APP/PS-1 mouse model, where retinal changes were evaluated. As in several studies in humans, evidence also shows that the retina is affected in AD animal models, including alterations in ERGs (Perez *et al*, 2009), RGCs degeneration (Williams *et al*, 2013) increased levels of APP, Aβ deposition and hyperphosphorylated tau protein (Ning *et al*, 2008; Liu *et al*, 2009; Gupta *et al*, 2016), and an increase in gliosis (Dinet *et al*, 2012; Edwards *et al*, 2014).

Nevertheless, retinal research is still in progress to provide more consistent and convergent data in AD context. However, despite the existence of conflicting results in both human and animal studies, there is no doubt that the retina is affected in AD.

1.2.3. Retina as a window to the brain

In fact, the eye is the only extension of the CNS that is not encased in the skull which favors the visualization of neural integrity more easily than in the brain. Taking into account the evidences previously described and assuming that retinal changes may reflect those that occur in a brain, retinal research represents an interesting, inexpensive and less invasive portal for studying not only the AD but also other neurodegenerative disorders.

Curiously, William Shakespeare once said “the eyes are the window to your soul” but in light of the current knowledge, it seems to be rightful to ask whether they can also be the window to the brain. Indeed, the last evidences showing visual changes, particularly in the retina, resembling to those found in the changing brain in AD led us to the concepts of the retina as a window to look into the brain or a mirror of the brain, which have gaining increasing attention in recent years given the obvious advantages that makes the retina a convenient research model for several neurodegenerative diseases. However, although this concept is not entirely novel, it was never properly explored since previous studies focused mainly in the brain or in the retina and only in a few studies, both retina and brain were assessed but with many limitations (Hart *et al*, 2016).

1.3. Missing links between brain and retina in the context of AD

Given the evidences demonstrating that the retina can be affected in AD, modern non-invasive optical imaging techniques can be potentially used for the early and cheaper detection of prospective biomarkers during the pre-clinical stages of AD. They may allow a better and more accurate diagnosis, monitor disease progression and evaluate response to therapies. However, there are still many missing links regarding the alterations that occur in the brain and retina of AD patients due to the lack of longitudinal and integrative studies investigating, at similar timepoints, changes on both regions. Although the several findings achieved in this area, it is still impossible to integrate and consequently understand how changes found in the retina and the brain correlate in AD, remaining several open questions that need to be solved. Thus, there is a need of performing a study that evaluates a set of biological parameters that will help to understand whether indeed the retina mirrors the changes in the brain, whether the molecular, cellular and physiological changes occur first in the retina or in the brain, which tissue is mostly affected and how changes progress along time.

Since the retina is a well-defined neuronal compartment, it can be isolated in an intact form and used to study molecular players involved in neuropathological disorders as well as the brain allowing establishing correlations between feature changes of both structures related to disease onset and progression.

Rationale and Aims

2. Rationale and Aims

Characterized by the extracellular accumulation of Aβ plaques followed by intracellular deposition of neurofibrillary tangles, AD is the most frequent neurodegenerative disorder with a huge global impact, however with no cure or efficient treatments. These features detected in AD patients lead to a massive neuronal loss and brain homeostasis disruption that may account some of the clinical manifestations observed in AD such as decline of memory and learning. However, these cognitive symptoms arise only after the occurrence of significant neuronal deterioration and AD diagnosis is complex, relying on expensive and invasive methods.

Given that, clinically, AD patients complain of frequent visual disturbances such as color discrimination, depth perception, contrast consciousness and comprehending structure from motion even before AD diagnosis, a new concept emerged and claims the eye, particularly the retina, as a window to the brain. In fact, the retina makes part of CNS and previous studies have shown that this structure displays several changes in many neurodegenerative disorders. Based on these evidences, the retina became an interesting research tool for many brain diseases. However, there are many missing links and open questions regarding the alterations occurring in these two regions that preclude us from looking at the retina as a reliable window or mirror of what happens in the brain, in the context of AD (Madeira *et al*, 2015a). Considering this data, in this work, we aimed:

- ► To clarify whether the retina can in fact mirror AD brain pathology, focusing on the early molecular and cellular changes occurring in both retina and brain. This would be essential to use the retina as a reliable window/mirror of the brain pathology for the early diagnosis of AD;
- ► To characterize the retinal changes in the early stages of disease phenotype in the 3xTg-AD model;
- ► To assess when alterations start appearing in both regions, which of them are mostly affected and how changes progress;
- ► To identify potential drug targets for the development of new treatments for AD.

In order to elucidate these issues, we carried out an integrative and longitudinal study, using the retina and the brain of an animal model of AD (3xTg-AD). We took advantage of the many changes described in AD brain including protein aggregates, synaptic loss, glial reactivity and hypometabolism to select a wide range of biological parameters and perform an extensive evaluation in hippocampus, cortex and retina from 3xTg-AD animal model and the age-matched wild-type (WT) animals (C57BL6/129S) in two early timepoints related with disease onset (4 and 8 months).

Experimental Procedure

3. Experimental Procedure

3.1. Reagents

Table 1 | Reagents.

Reagents	Supplier
4',6'-diamidino-2-phenylindole (DAPI)	Life Technologies
Bovine serum albumin (BSA)	NZYTech
Cell Lysis buffer	Cell Signaling
cOmplete™, EDTA-free Protease Inhibitor	Sigma-Aldrich
Dithiotreitol (DTT)	Sigma-Aldrich
Enhanced chemifluorescent (ECF) substrate	GE Healthcare
Enhanced chemiluminescence (ECL) substrate	Bio-Rad
Glycergel mounting medium	DAKO
WesternBright Sirius HRP substrate	GRISP
Fluorogenic β-secretase activity assay kit	Calbiochem | Millipore
Bicinchoninic acid (BCA) assay kit	Pierce Biotechnology | Thermo Scientific
DeadEnd™ Fluorometric TUNEL System	Promega
Goat Serum	Sigma-Aldrich
Isoflurane	Abbott Laboratories
Ketamine	Imalgene 1000
Low-fat dry milk	Nestle
Optimal Cutting Temperature (OCT) compound	Shadon Cryomatrix | Thermo Scientific
Paraformaldehyde (PFA)	Merk
Phenylmethanesulfonyl fluoride (PMSF)	Sigma-Aldrich
PhosSTOP™	Sigma-Aldrich
Triton X-100	Sigma-Aldrich
Xylazine	Ronpum

3.2. Animal model

Experiments were performed in 4- and 8-month-old 3xTg-AD mice harboring three human mutant genes namely *APP*$_{swe}$, *PSEN-1*$_{M146V}$ and *Tau*$_{P301L}$ and WT animals (C57BL6/129S) as age-matched controls. Animals were housed in certified local facilities, kept in standard housing conditions (22ºC and 55% relative humidity, dark/light cycle of 12 h, with lights on at 8:00 am) and were provided with food (standard rodent chow) and water *ad libitum*. During this study only male mice were used which were randomly assigned to each timepoint.

Procedures involving animals were conducted in accordance with the guidelines of the European Community directive for the use of animals in laboratory (2010/63/EU), translated to the Portuguese law in 2013 (Decreto-lei 113/2013), and in accordance with the Association for Research in Vision and Ophthalmology (ARVO) guidelines for the use of animals in vision research. The experiments were approved by Institutional Ethics Committee (Orgão Responsável pelo Bem-Estar Animal – ORBEA) (approval ID: 16-2015 IBILI).

3.3. Preparation of biological samples

Animals were placed under isoflurane anesthesia, sacrificed by cervical dislocation and both brain and eye tissues were immediately isolated. Cortex, hippocampus and retina were dissected in ice-cold Hank's balanced salt solution (HBSS: 137 mM NaCl, 5.4 mM KCl, 0.45 mM KH_2PO_4, 0.34 mM NaHPO, 4 mM $NaHCO_3$, 5 mM glucose, pH 7.4), frozen in liquid nitrogen and stored at -80ºC. Frozen samples used in Western Blotting and BACE activity assays were homogenized in cell lysis buffer from Cell Signaling supplemented with 0.1 mM PMSF, 2 mM DTT as well as protease and phosphatase inhibitor cocktails (PhosSTOP™ and cOmplete™, EDTA-free Protease Inhibitor, respectively). Samples from retina were sonicated (3 pulses, 2 seconds each), whereas the cortex and hippocampus were homogenized followed by three freezing and thawing cycles. The resulting homogenates were centrifuged at 16,100 × g for 10 min at 4ºC and the supernatants were stored at -80ºC until use. In the case of the samples used for measurement of mitochondrial enzymatic activities,

homogenization was made in lysis buffer containing 250 mM sucrose and 5 mM HEPES (2-[4-(2-hydroxyethyl)piperazin-1-yl]ethanesulfonic acid), pH 7.4.

The protein concentration was measured using the bicinchoninic acid (BCA) protein assay kit, following manufacturer's instructions.

3.4. Western Blotting in SDS-PAGE

After determining protein concentration, the samples were denatured by adding 6x concentrated sample buffer (0.5 M Tris-HCl, 10% SDS, 30% Glycerol, 0.6 M DTT, 0.012% bromophenol blue; pH 6.8) and heating for 5 min at 95ºC.

For each protein, different amounts of protein were tested (10, 20 and 40 μg) to select the proper amount to use. Samples were separated by sodium dodecyl sulfate-polyacrylamide gel electrophoresis (SDS-PAGE) using 8-15% polyacrylamide gels and a bicine-buffered solution (25 mM Tris-base, 25 mM bicine, 0.1% SDS, pH 8.3). Samples were stacked by running at 60 V for 15 min and resolved at 120 V for 1 h. Proteins were then electrophoretically transferred onto PVDF membranes (Millipore) at 750 mA for 90 min, using a CAPS-buffered (*N*-cyclohexyl-3-aminopropanesulfonic acid) solution with methanol (10 mM CAPS, 10% methanol, pH 11.0). Nonspecific binding was blocked by incubating the membranes with 5% BSA (or 5% low-fat dry milk) in Tris-buffered saline (20 mM Tris-HCl, 137 mM NaCl, pH 7.6) containing 0.1% Tween-20 (TBS-T) for 1 h at room temperature (RT). The membranes were then incubated with the appropriate primary antibody (Table 2) diluted in TBS-T with 5% BSA (or 1% low-fat dry milk), overnight at 4ºC and more 1 h in the day after at RT. After three 15 min washes in TBS-T, membranes were incubated with secondary antibodies (Table 2) conjugated with horseradish peroxidase (HRP) or alkaline phosphatase (AP) for 90 min at RT and washed again with TBS-T. Membranes were processed for detection using the ECL or ECF substrate and visualized on ImageQuantTM LAS 500 (GE Healthcare) or Typhon FLA 900 (GE Healthcare) respectively. At the end, membranes were re-incubated for β-actin to prove that similar amounts of protein were applied to the gels. Bands were quantified using Bio-Rad Quantity One Analysis software and data are presented as a ratio between the

immunoreactivity of target protein and β-actin and are expressed as percentage of control.

Table 2 | Primary and secondary antibodies used in Western Blotting.

	Antibody	Host	Protein (µg)	Dilution	Supplier (Cat no)
Primary Antibodies	Anti-Amyloid-β (D54D2)	Rabbit	20	1:1,000	Cell Signaling (#8243)
	Anti-Amyloid-β (6E10)	Mouse	50 (only in the retina)	1:1,000	BioLegend (SIG-39320)
	Anti-p-tau (ser^{396})	Rabbit	10	1:1,000	Santa Cruz (sc-101815)
	Anti-APP	Rabbit	20	1:1,000	Sigma-Aldrich (A8717)
	Anti-BACE	Rabbit	20	1:1,000	Cell Signaling (#5606)
	Anti-Syntaxin	Mouse	10	1:5,000	SYSY (110 011C3)
	Anti-Synaptophysin	Mouse	10	1:1,000	Sigma-Aldrich (S5768)
	Anti-ChAT	Goat	20	1:1,000	Millipore (AB144P)
	Anti-GFAP	Mouse	20	1:5,000	Millipore (IF03L)
	Anti-Vimentin	Rabbit	15	1:1,000	Abcam (ab92547)
	Anti-β-Actin	Rabbit	-	1:5,000	Sigma-Aldrich (A2066)
	Anti-β-Actin	Mouse	-	1:5,000	Sigma-Aldrich (A5441)
Secondary Antibodies	AP Anti-Mouse IgG	Goat	-	1:1,0000	Sigma-Aldrich (A3562)
	AP Anti-Rabbit IgG	Goat	-	1:1,0000	Sigma-Aldrich (A3687)
	HRP Anti-Goat	Rabbit	-	1:1,0000	Alfagene (611620)
	HRP Anti-Mouse	Goat	-	1:1,0000	Bio-Rad (#170-6516)
	HRP Anti-Rabbit	Goat	-	1:1,0000	Bio-Rad (#170-6515)

3.5. BACE activity assay

The fluorogenic β-secretase activity assay kit was used to measure BACE activity in WT and 3xTg-AD mice cortex, hippocampus and retina according to the manufacturer's instructions.

Firstly, 48 µL of Reaction Buffer and 2 µL of β-secretase substrate supplied in dimethyl sulfoxide, provided with the kit, were added to 50 µL of the tissue samples in a 96-well plate. Positive control (48 µL Extraction Buffer, 2 µL Active β-secretase, 48 µL Reaction Buffer and 2 µL β-secretase substrate) and background control (49 µL Extraction Buffer, 49 µL Reaction Buffer and 2 µL β-secretase substrate) were also added to the plate. The reaction was carried out for 2 h in the dark at 37ºC and the fluorescence was measured in SpectraMax Gemini EM fluorescence plate reader (Molecular Devices) using an excitation wavelength of 345 nm and an emission wavelength of 505 nm. Background reading from substrate and buffers were subtracted from samples, and β-secretase activity was expressed as relative fluorescence units (RFU) per µg of protein.

3.6. Measurement of mitochondrial enzymatic activities

3.6.1. Citrate Synthase activity

Citrate synthase activity was determined as previously described by Coore and colleagues (Coore *et al*, 1971), with slight modifications. Briefly, 25-50 µg of samples from hippocampal, cortical and retinal homogenates, obtained as previously described, were incubated at 37°C in a reaction buffer containing 100 mM Tris, 200 µM Acetyl-CoA, and 200 µM 5,5′-dithiobis-2-nitrobenzoic acid, pH 8.0. Enzymatic activity was determined in a SpectraMax plus 384 microplate reader (Molecular Devices), at 37°C, by following the increase in absorbance (412 nm) upon addition of 100 µM freshly-prepared oxaloacetate. Enzyme activity was calculated through the mean of the slopes of duplicates obtained during the linear phase. Citrate synthase-specific activity was calculated by subtracting the basal activity in the presence of 0.1% Triton-X 100. A molar extinction coefficient of ε_{412} = 13.6 $mM^{-1}.cm^{-1}$ and normalization to protein

amount were applied. Enzyme activity was expressed as nmol of oxaloacetate min^{-1}.mg $protein^{-1}$.

3.6.2. NADH-ubiquinone oxidoreductase (Complex I) activity

Complex I activity was determined by modification of a method previously described by Long and collaborators (Long *et al*, 2009). Briefly, 15-50 μg of tissue homogenate, obtained as previously described, was diluted in reaction buffer containing 25 mM KH_2PO_4, 5 mM $MgCl_2$, 300 μM KCN, 4 μM antimycin A, 3 $mg{\cdot}mL^{-1}$ BSA, 60 μM coenzyme Q_1, 160 μM and 2,6-dichlorophenolindophenol (DCPIP), pH 7.5. Complex I activity was measured in a spectrophotometer (SpectraMax plus 384) at 37ºC by following the decrease in absorbance (600 nm) of DCPIP upon addition of 100 μM freshly-prepared NADH. Enzyme activity was calculated through the mean of slopes of duplicates, obtained during the linear phase. Mitochondrial complex I specific activity was determined as the difference between basal activity in the absence or presence of 10 μM rotenone (specific inhibitor of complex I). A molar extinction coefficient of ε_{600} = 19.1 $mM^{-1}.cm^{-1}$ and normalization to protein amount were applied. Complex I activity was expressed as nmol DCPIP min^{-1}.mg $protein^{-1}$. Finally, mitochondrial complex I enzymatic activity was normalized to citrate synthase activity.

3.6.3. Cytochrome c oxidase (Complex IV) activity

Complex IV activity was determined by modification of a method previously described by Brautigan and collaborators (Brautigan *et al*, 1978). Briefly, 25-15 μg of tissue homogenate, obtained as previously described, was incubated at 37°C, in reaction buffer containing 50 mM KH_2PO_4, 4 μM antimycin A and 0.05% n-dodecyl-β-d-maltoside, pH 7.0. Enzymatic activity was followed by a decrease in absorbance of reduced cytochrome c (cyt c_{red}) at 550 nm, upon addition of 57 μM freshly-prepared cyt c_{red} in a spectrophotometer (SpectraMax plus 384). Enzyme activity was calculated through the mean of slopes of duplicates, obtained during the linear phase. Mitochondrial complex IV specific activity was determined as the difference between basal activity in the absence or presence of 10 mM of KCN (complex IV specific inhibitor). A molar extinction coefficient of ε_{550} = 19.1 $mM^{-1}.cm^{-1}$ and normalization to

protein amount were applied. Activity was expressed as nmol cyt c_{red} min^{-1}.mg $protein^{-1}$. Finally, mitochondrial complex IV enzymatic activity was normalized to citrate synthase activity.

3.6.4. Aconitase activity

Aconitase activity was determined as previously described by Krebs and Holzach (Krebs & Holzach, 1952), with slight modifications. Briefly, 15-50 μg of tissue homogenate, obtained as previously described, was diluted in reaction buffer containing 50 mM Tris-HCl and 0.6 mM $MnCl_2$, pH 7.4, followed by one freezing and thawing cycle. Then, samples were centrifuged at 16,100 × g for 3 min and aconitase activity was immediately measured in a spectrophotometer (Spectramax plus 384) at 240 nm, monitoring the cis-aconitase levels after the addition of 20 mM freshly-prepared isocitrate, at 25ºC. Enzyme activity was calculated through the mean of slopes of duplicates, obtained during the linear phase. A molar extinction coefficient of ε_{240} = 3.6 $mM^{-1}.cm^{-1}$ and normalization to protein amount were applied. Aconitase activity was expressed as $U.min^{-1}$.mg $protein^{-1}$. One unit was defined as the amount of enzyme necessary to produce 1 μM cis-aconitate per minute.

3.7. Preparation of frozen tissue sections

Animals were anaesthetized with an intraperitoneal injection of ketamine (90 mg/kg) and xylazine (10 mg/kg) and intracardially perfused with phosphate-buffered saline (PBS; 137 mM NaCl, 2.7 mM KCl, 10 mM Na_2HPO_4 and 1.8 KH_2PO_4, pH 7.4) followed by 4% (w/v) paraformaldehyde in 0.1 M PBS. The brains were dissected and then kept in 4% PFA until being transferred in the next day to a 30% sucrose solution in PBS overnight at 4ºC and frozen at -80ºC. Coronal sections with 30 μm thickness were cut, at the level of hippocampus, using a cryostat (Leica CM3050S, Leica Biosystems) set at -21ºC and -20ºC, for the chamber and object temperature, respectively. The slices were transferred to 24 well plates filled with cryoprotection solution (50 mM $NaH_2PO_4.H_2O$, 50 mM K_2HPO_4, 30% sucrose, 30% ethylene glycol, pH 7.2) and stored at 4ºC.

Eyes were post-fixed in 4% PFA for 1 h and after removing the cornea, they were fixed for an additional 1 h in 4% PFA. After washing in PBS, the tissue was transferred

to 15% sucrose solution in PBS for 1 h, followed by 30% sucrose in PBS overnight at 4ºC. Finally, they were embedded in optimal cutting temperature medium with 30% of sucrose in PBS (1:1) for 15 min and frozen at -80ºC before sectioning. With chamber and object cryostat temperature set at -27ºC and -26ºC, respectively, 16 µm sections were obtained only from the right eyes, placed directly on Superfrost Plus glass slides (Menzel-Glaser | Thermo Scientific) and stored at -20ºC until use.

3.8. Fluorescence immunohistochemistry

The methodology behind immunohistochemistry (IHC) procedure may be quite different depending on the tissue nature. Being both brain and retina anatomically distinct, two immunohistochemical staining procedures were performed based on proper tissue context.

3.8.1. Retinal cryosections

Retinal slices, previously mounted on glass slides, were let to thaw at RT overnight. The sections were then fixed with ice-cold acetone at -20ºC for 10 min followed by rehydration in PBS twice until the removal of OCT. Before the follow steps, each retinal section was surrounded with a hydrophobic pen (DAKO Pen, LusoPalex). Cryosections were then permeabilized with 0.25% Triton X-100 in PBS for 30 min followed by blocking in 10% Normal Goat Serum and 1% BSA in PBS for additional 30 min at RT in a humid atmosphere, to avoid tissue dehydration. The slices were then incubated overnight at 4ºC with primary antibodies (Table 3) diluted in PBS with 1% BSA. After washing in PBS, 10 min each, the sections were incubated with proper secondary antibody (Table 3) and nuclear dye DAPI (1:5,000) for 1 h at RT, in the dark, and washed again three times with PBS. Finally, the slices were mounted with DAKO Glycergel mounting medium. The preparations were observed and images for analyses were acquired in a fluorescence microscope Zeiss Axio Imager 2, using a 20x objective lens (Plan Apochromat 20x/0.8), and processed by Zen Blue software (Zeiss Microscopy). Representative images were acquired with a laser scanning confocal microscope LSM 710 META connected to ZEN Black software (Zeiss Microscopy),

using a 40x objective lens (oil immersed, EC Plan-Neofluar 40x/1.30 Oil DIC M27 objective).

3.8.2. Free-floating brain sections

Free-floating brain sections located at the stereotaxic coordinates of intraneural 1.98 mm and bregma -1.82 mm (Paxinos et al. 2004) (Figure 7) were selected and washed three times with PBS for 10 min each. All wash and incubation times were

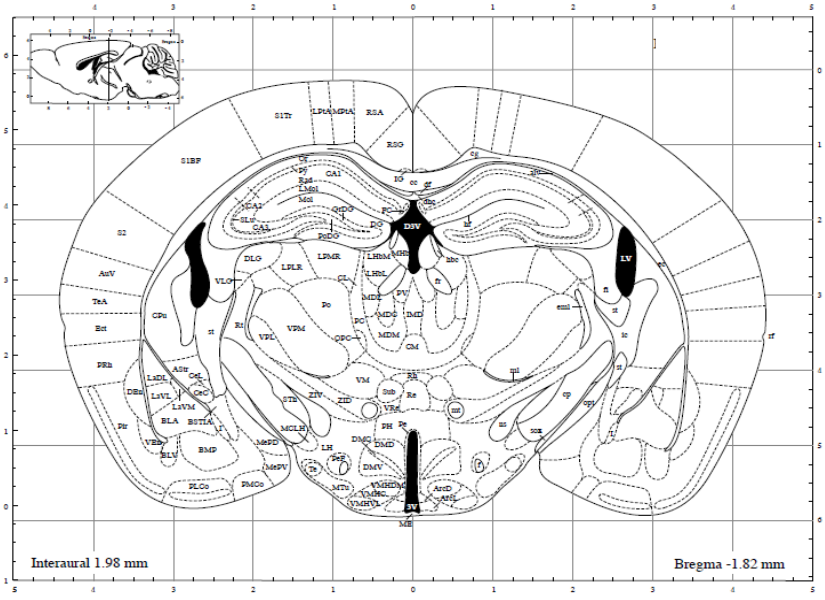

Figure 7 | Representative image of the mouse brain in the analyzed section (from Paxinos et al. 2004).

performed in mild agitation. Slices were then incubated with a permeabilization and blocking solution composed of PBS containing 5% BSA and 0.1% Triton X-100 at RT for 2 h to improve specific binding. Primary antibodies were diluted in the same solution and slices incubated at 4ºC for 48 h (Table 3). Thereafter, brain slices were washed three times in PBS followed by incubation with corresponding secondary antibodies and DAPI (1:5,000) for 2 h at RT (Table 3). Notice that secondary antibodies solutions were previously centrifuged for 20 min at 16,100 × g at 4ºC, in order to precipitate antibody aggregates avoiding the excess of background. After washing again, slices were mounted on gelatinized microscope slides using DAKO glycergel mounting medium. Sections were kept in the dark at 4ºC, until performing image acquisition with a fluorescence microscope Zeiss Axio Imager 2, using a 40x objective

lens (Plan Apochromat 20x/0.8), and processed by Zen Blue software (Zeiss Microscopy). Representative images were acquired with a laser scanning confocal microscope LSM 710 META connected to ZEN Black software (Zeiss Microscopy), using a 40x objective lens (oil immersed, EC Plan-Neofluar 40x/1.30 Oil DIC M27 objective).

Table 3 | Primary and secondary antibodies used in immunohistochemistry for retinal and brain sections.

	Antibody	Host	Dilution	Supplier (Cat no)
Primary Antibodies	Anti-Iba1	Rabbit	1:1,000	Wako (#019-19741)
	Anti-OX-6	Rat	1:500	eBioscience (14-5321)
	Anti-Vimentin	Rabbit	1:500	Abcam (ab92547)
	Anti-GFAP	Chicken	1:500 (retina) 1:2000 (brain)	Millipore (AB5541)
	Anti-Amyloid-β (6E10)	Mouse	1:500	BioLegend (SIG-39320)
	Anti-PHF-1	Mouse	1:1,000	Gentle gift from Paula Moreira Lab
Secondary Antibodies	Alexa Fluor 488 Anti-Rabbit IgG	Goat	1:500	Invitrogen (A11008)
	Alexa-Fluor 488 Anti-Mouse IgG-	Goat	1:500	Invitrogen (A11001)
	Alexa-Fluor 568 Anti-Rabbit IgG-	Goat	1:500	Invitrogen (A11036)
	Alexa-Fluor 568 Anti-Mouse IgG-	Goat	1:500	Invitrogen (A11004)
	Alexa-Fluor 568 Anti-Chicken IgG-	Goat	1:500	Invitrogen (A11041)
	Alexa Fluor 568 Anti-Rat IgG	Goat	1:500	Invitrogen (A11077)

3.8.3. Terminal deoxynucleotidyl transferase (TdT)-mediated dUTP nick end labeling (TUNEL) assay

DNA fragmentation was detected using DeadEnd™ Fluorometric TUNEL System, according to the manufacturer instructions. Brain slices were placed on gelatinized microscope slides and such as retinal sections, both were let to dry overnight at RT.

Tissue sections were fixed with 4% paraformaldehyde for 15 min and then washed twice in PBS, 5 min each time. Then, sections were permeabilized for 10 min

with 20 μg/mL proteinase K solution. After washing twice in PBS, the sections were covered with equilibration buffer (200 mM potassium cacodylate, 25 mM Tris-HCl, 0.2 mM DTT, 0.25 mg/mL BSA and 2.5 mM cobalt chloride) for 10 min at RT. After removing the excess of solution, sections were incubated with recombinant TdT enzyme buffer (a mix of equilibration buffer with TdT enzyme and nucleotide mix containing dUTP conjugated to fluorescein) at 37ºC. After 1 h, the reaction was stopped by immersing the slides in saline-sodium citrate buffer (175g/L NaCl, 88.1 g/L sodium citrate) for 15 min. Tissue sections were washed twice in PBS, 5 min each time, followed by incubation with DAPI (diluted 1:5,000) and washed again in PBS. A positive control was also performed by treating both retinal and brain section with DNaseI causing DNA fragmentation. At the end, sections were mounted using DAKO glycergel mounting medium, covered with coverslips, sealed with transparent nail polish and kept in the dark at 4ºC. The preparations were observed and images for analyzes were acquired in a fluorescence microscope Zeiss Axio Imager 2, using a 20x objective lens (Plan Apochromat 20x/0.8), and processed by Zen Blue software (Zeiss Microscopy). Representative images were acquired with a laser scanning confocal microscope LSM 710 META connected to ZEN Black software (Zeiss Microscopy), using a 40x objective lens (oil immersed, EC Plan-Neofluar 40x/1.30 Oil DIC M27 objective).

3.9. Statistical analysis

The statistical analysis was carried out in GraphPad Prism version 6 (GraphPad Software Inc.). All graphic values are expressed as mean ± standard error of the mean (SEM). Differences between two independent groups were analyzed by Student's t-test. To assess differences between more than two groups, a non-parametric Kruskal-Wallis ANOVA test followed by Dunn's multiple comparison test was performed. Statistical significance was considered at $p<0.05$.

Results

4. Results

Given the urgent need to perform an integrative study able to provide accurate and reliable information regarding the alterations that occur in AD not only in the brain but also in the retina, we assessed a large set of molecular and cellular parameters using isolated biological samples from 3xTg-AD animal model harboring the three human mutant genes aforementioned. All parameters described below were analyzed in the hippocampus, cortex and retina at two early timepoints (4 and 8 months) to clarify when alterations start appearing in the brain and retina and how they develop as the disease progresses.

4.1. Alterations in key molecular players involved in AD pathophysiology

Being considered major hallmarks of AD, Aβ and p-tau are well described as presenting significant increased levels in AD brain, thus having a large tendency to aggregate and form deposits harmful to the proper functioning of the brain and neural connections. We started by evaluating the protein content, by Western blotting (WB), of Aβ and p-tau as well as of APP and BACE, two of the main molecular players in AD that contribute to Aβ increased levels.

4.1.1. Aβ and p-tau protein levels increase in the hippocampus and cortex of 3xTg-AD mice

At the earliest timepoint (4 months) we found a significant increase, comparing with control mice, in the levels of Aβ monomers in 3xTg-AD mice in both hippocampus (288.0 ± 57.2% of WT, $p<0.001$) and cortex (220.2 ± 37.7% of WT, $p<0.001$), that persisted and increased even more at 8 months in hippocampus (615.0 ± 164.0% of WT, $p<0.05$) and cortex (697.8 ± 91.4%, $p<0.0001$) (Figure 8A and B). However, the same amount of protein loaded in the gel used for hippocampal and cortical samples was not enough to detect Aβ in the retinal homogenates, being necessary to increase significantly the quantity of protein loaded in the gel. Since the amount of retinal tissue is limited, which brings difficulties for the assessment of all proteins under study, we performed just one WB, loading 50 μg of protein, to check whether we could

detect Aβ in the retina, using samples from WT and 3xTg-AD mice at 4 and 8 months of age. For that, we used the antibody anti-amyloid-β (clone D54D2) previously used and the antibody anti-amyloid-β_{1-16} (clone 6E10) (Figure 8C).

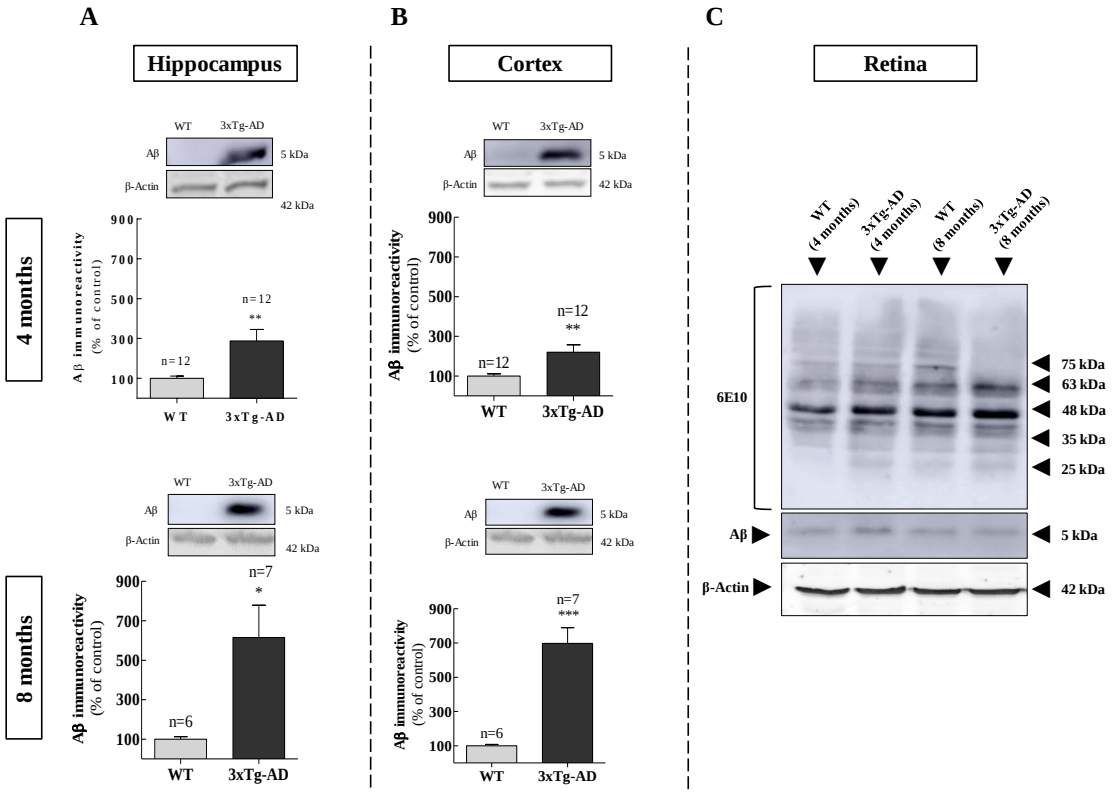

Figure 8 | Aβ levels are increased in the hippocampus and cortex of 3xTg-AD mice at 4 and 8 months of age. Aβ protein levels were evaluated in the hippocampal **(A)** and cortical **(B)** homogenates from 3xTg-AD and WT mice at 4 and 8 months old, by Western blotting.
Representative images of protein blots are presented above the respective graph as well as the number of animals used. Results are expressed as mean ± SEM and represent the percentage (%) of WT animals. Statistical significance was assessed by Student's t-test: *p<0.05, **p<0.01, ***p<0.001, different from control.
Membrane showing the presence of Aβ protein (detected with antibody anti-amyloid-β (clone D54D2) and the antibody anti-amyloid-β_{1-16} (clone 6E10)) in the retina from 3xTg-AD and WT mice at 4 and 8 months old by Western blotting **(C).**

Regarding p-tau levels, they were significantly increased at 4 months of age in the 3xTg-AD model not only in the hippocampus (203.2 ± 37.3% of WT, p<0.001) and cortex (185.2 ± 27.0% of WT, p<0.001) but also in the retina (151.2 ± 12.8% of WT, p<0.001). This increase only persisted until 8 months in the hippocampus (224.8 ± 28.0% of WT, p<0.001) (Figure 9A, B and C).

Changes detected in both Aβ and p-tau protein levels in hippocampus, cortex and retina were recapitulated by immunohistochemistry evaluation (data not shown).

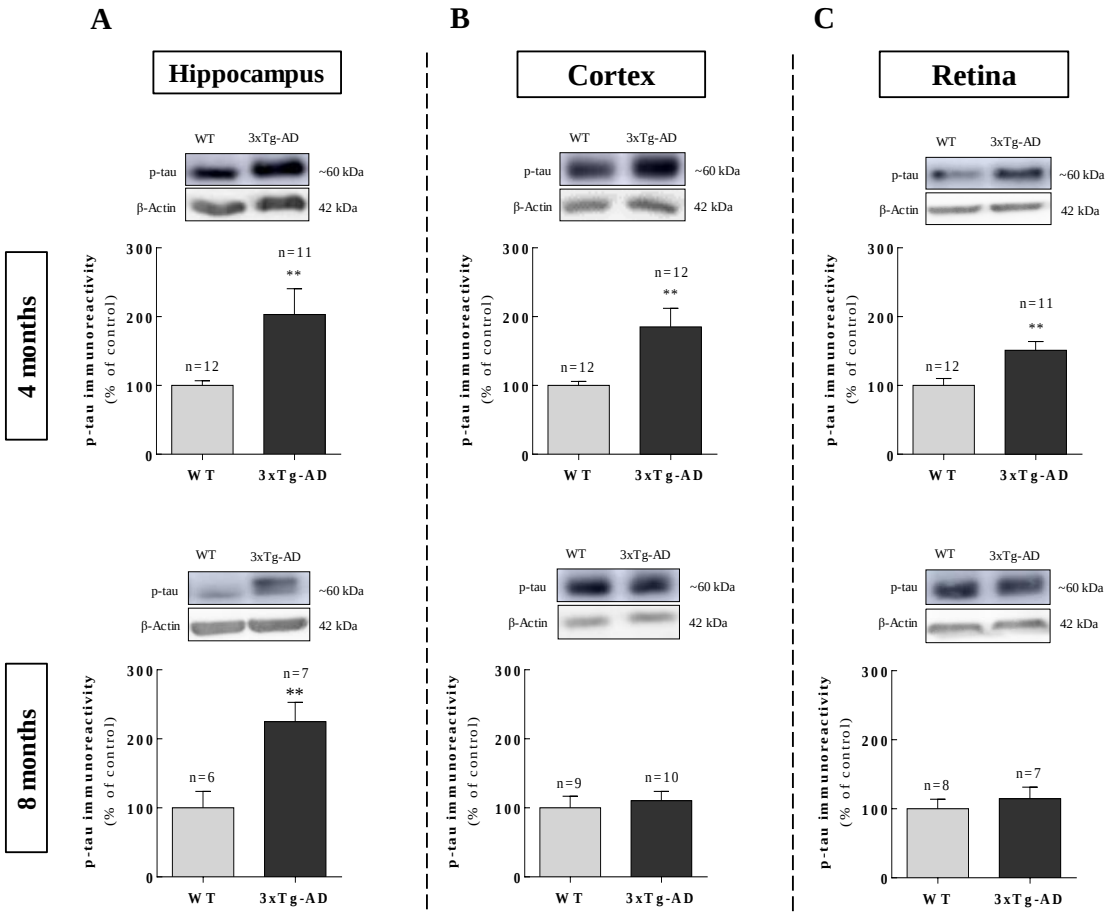

Figure 9 | p-tau protein levels increased in hippocampus, cortex and retina of 3xTg-AD mice at 4 months of age. p-tau protein levels were evaluated in the hippocampal **(A)**, cortical **(B)** and retinal **(C)** homogenates from 3xTg-AD and WT mice at 4 and 8 months old, by Western blotting.
Representative images of protein blots are presented above the respective graph as well as the number of animals used. Results are expressed as mean ± SEM and represent the percentage (%) of WT animals. Statistical significance was assessed by Student's t-test: **p<0.01, different from control.

4.1.2. The protein levels of APP increase in the hippocampus of 3xTg-AD mice at 8 months

No change in the APP protein content was noted in any of the analyzed regions at 4 months of age in the 3xTg-AD mice, comparing to WT animals. Nevertheless, their levels significantly increased in the hippocampus (147.2 ± 6.2% of WT, p<0.0001) at 8 months (Figure 10A).

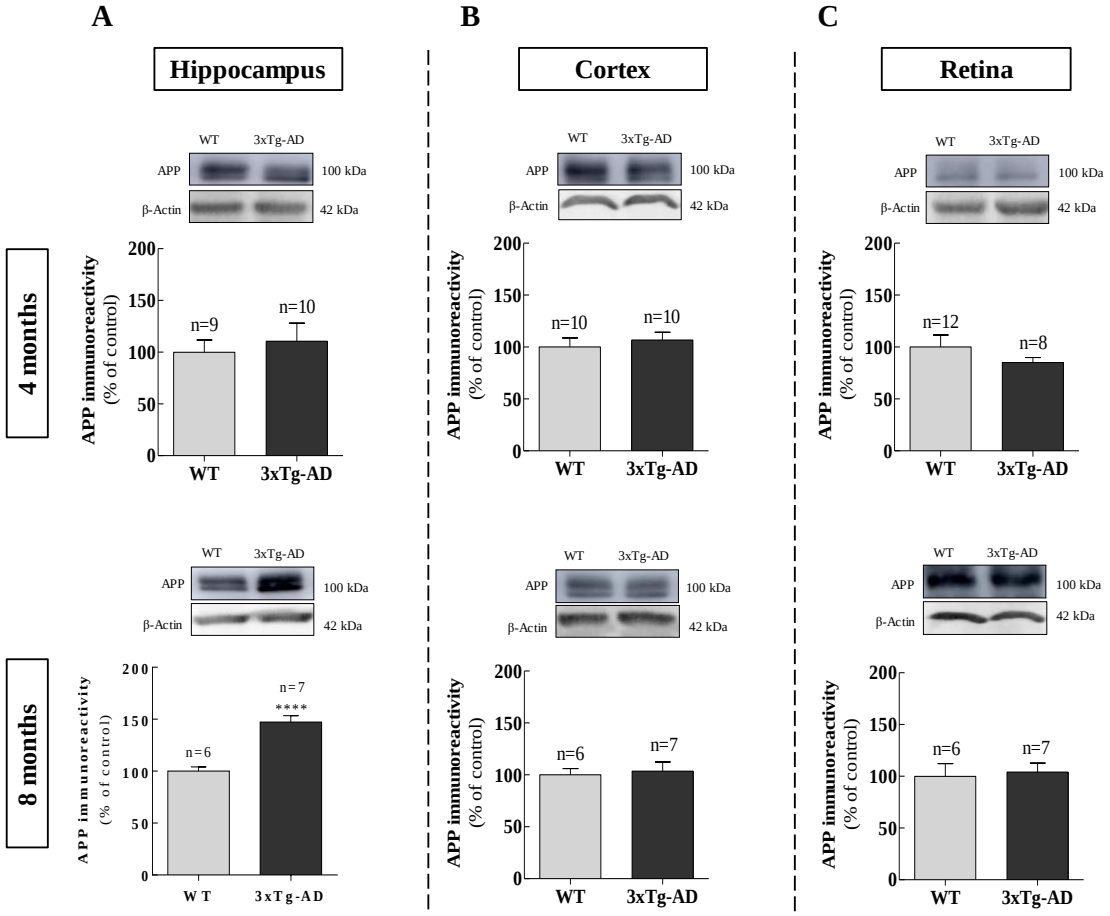

Figure 10 | The protein levels of APP increase in the hippocampus of 3xTg-AD mice at 8 months. APP protein levels were evaluated in the hippocampal **(A)**, cortical **(B)** and retinal **(C)** homogenates from 3xTg-AD and WT mice at 4 and 8 months old, by Western blotting.
Representative images of protein blots are presented above the respective graph as well as the number of animals used. Results are expressed as mean ± SEM and represent the percentage (%) of WT animals. Statistical significance was assessed by Student's t-test: ****p<0.0001, different from control.

4.1.3. The protein levels and activity of BACE are not changed in the brain and retina of 3xTg-AD mice at 4 and 8 months

Regarding the protein levels of BACE, the enzyme that cleaves APP, thus initiating the amyloidogenic pathway, we did not detect any difference between transgenic and control mice in the hippocampus, and cortex and retina at 4 and 8 months (Figure 11A, B and C). Given that from 4 months there is a significant increase in the Aβ levels in the hippocampus and cortex but the protein content of BACE remains unchanged, we performed a BACE activity assay. Surprisingly, we did not find differences between transgenic and control mice neither in the hippocampus nor in the cortex at 4 and 8 months (Figure 11D and E). No changes were also detected in BACE activity in the retina as well (Figure 11F).

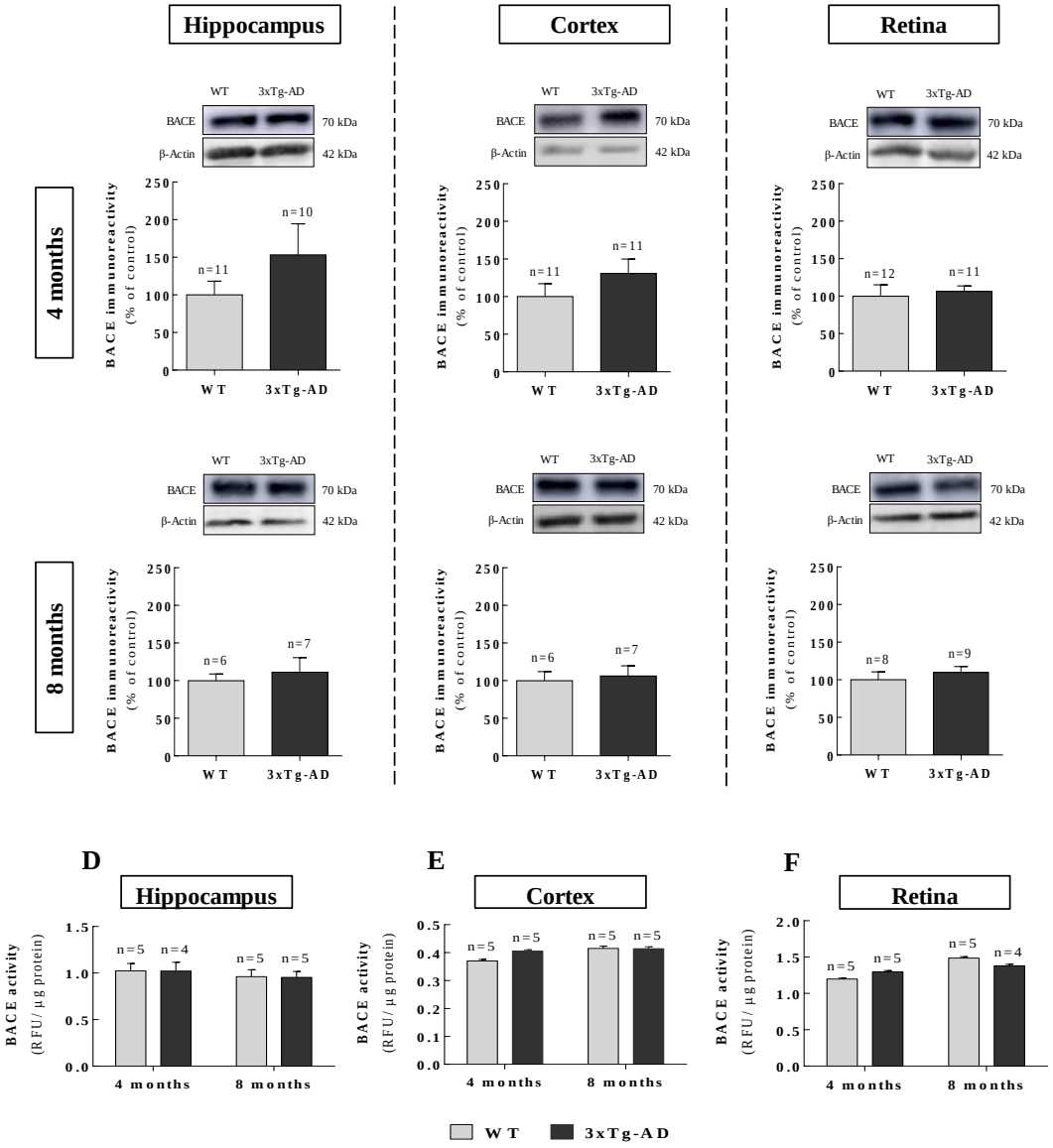

Figure 11 | The protein levels and enzymatic activity of BACE are not changed in the brain and retina of 3xTg-AD mice at 4 and 8 months. BACE protein levels were evaluated in the hippocampal **(A)**, cortical **(B)** and retinal **(C)** homogenates from 3xTg-AD and WT mice at 4 and 8 months old, by Western blotting.

Representative images of protein blots are presented above the respective graph as well as the number of animals used. Results are expressed as mean ± SEM and represent the percentage (%) of WT animals. Statistical significance was assessed by Student's t-test.

BACE activity was assessed in the hippocampus **(D)**, cortex **(E)** and retina **(F)** homogenates from 3xTg-AD and WT mice at 4 and 8 months old, by enzymatic assay. Above each bar is indicated the number of animals used. Results were expressed as relative fluorescence unit (RFU) per µg of protein, as mean ± SEM. Statistical significance was assessed by Kruskal–Wallis ANOVA test followed by Dunn's multiple comparison test.

4.2. Assessment of synaptic dysfunction and neuronal loss

Knowing that alterations in Aβ and p-tau protein levels trigger a cascade of events that can lead to synaptic dysfunction and neuronal loss impairing the neuronal network, we first analyzed, by WB, the levels of two synaptic proteins, syntaxin and synaptophysin (synaptic integrity markers) which are present in pre-synaptic neurons and in pre-synaptic vesicles, respectively, playing both an important role in proper synaptic function. Then, we also checked by WB the levels of the enzyme ChAT, which is responsible for catalyzing the transfer of an acetyl group from the acetyl-CoA to choline yielding the neurotransmitter ACh. This enzyme is found in cholinergic neurons which are one of the most affected neurons in AD, presumably because of the reduction of ChAT content. We also evaluated cell death by TUNEL assay in the three regions under study.

4.2.1. Syntaxin and synaptophysin protein levels are not consistently altered in 3xTg-AD mice

The levels of syntaxin significantly increased in the cortex of 3xTg-AD mice comparing to WT animals at 4 months of age (198.0 ± 22.6 of WT, $p<0.05$). However, this increase did not persist at 8 months (Figure 12B). The levels of syntaxin were not affected in the hippocampus and retina of 3xTg-AD mice at both (Figure 12A and C).

Regarding synaptophysin, no significant alterations were found in the hippocampus, cortex and retina of 3xTg-AD mice. However, there is a tendency for a decrease in synaptophysin in the cortex at 8 months (74.9 ± 7.0% of WT, $p=0.1066$) (Figure 12E).

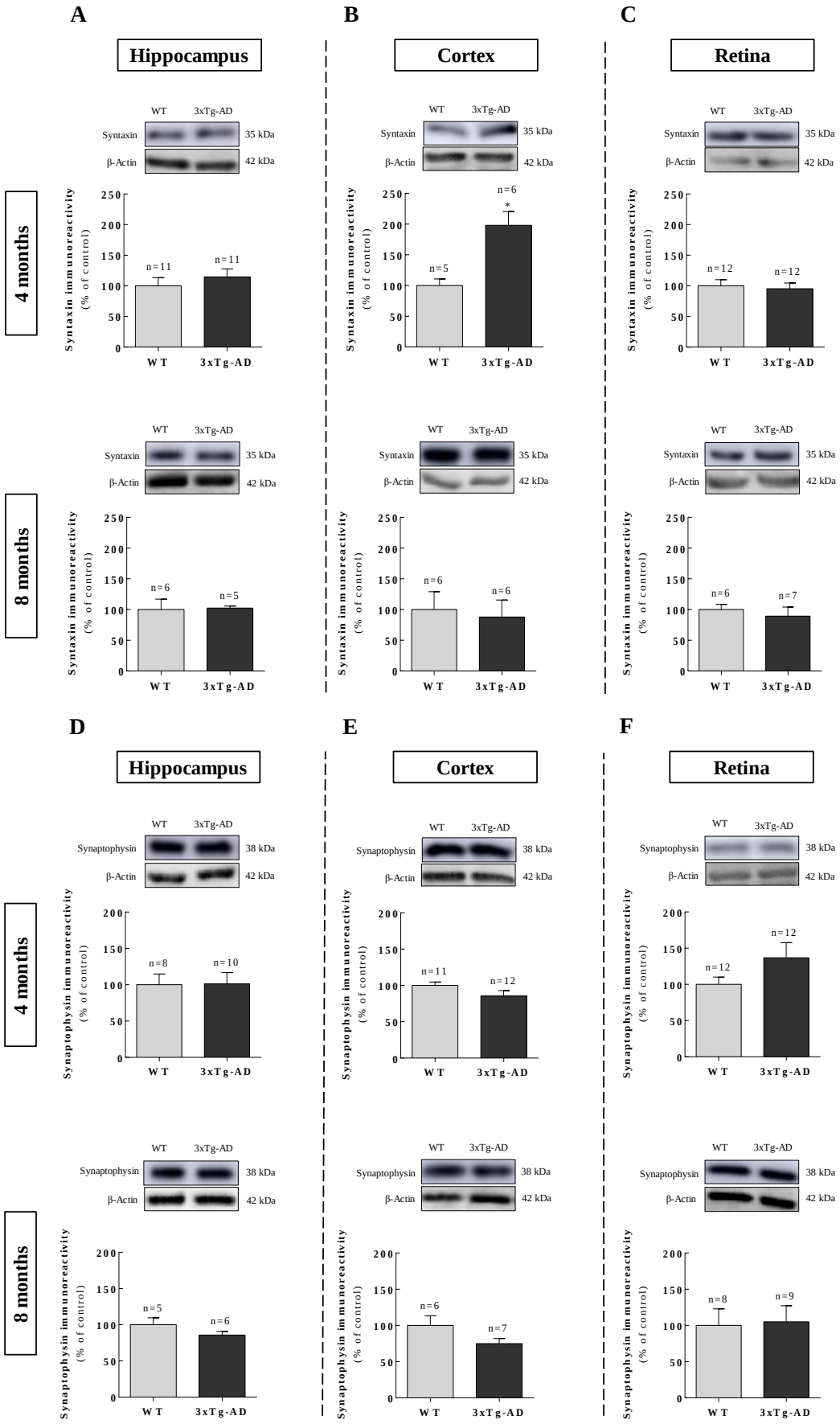
A
B
C
Hippocampus
Cortex
Retina
4 months
8 months
WT
3xTg-AD
Syntaxin
β-Actin
35 kDa
42 kDa
Syntaxin immunoreactivity (% of control)
n=11
n=11
n=5
n=6
*
n=12
n=12
n=6
n=5
n=6
n=6
n=6
n=7
D
E
F
Synaptophysin
38 kDa
Synaptophysin immunoreactivity (% of control)
n=8
n=10
n=11
n=12
n=12
n=12
n=5
n=6
n=6
n=7
n=8
n=9
WT
3xTg-AD

Figure 12 | The protein levels of syntaxin and synaptophysin are not consistently altered in 3xTg-AD mice. The protein levels of syntaxin and synaptophysin were evaluated in the hippocampal **(A, D** respectively**)**, cortical **(B, E** respectively**)** and retinal **(C, F** respectively**)** homogenates from 3xTg-AD and WT mice at 4 and 8 months old, by Western blotting.
Representative images of protein blots are presented above the respective graph as well as the number of animals used. Results are expressed as mean ± SEM and represent the percentage (%) of WT animals. Statistical significance was assessed by Student's t-test: *p<0.05, different from control.

4.2.2. The protein levels of ChAT remain unchanged in 3xTg-AD mice 4 and 8 months of age

Regarding the protein content of ChAT, no significant differences were found in the three regions assessed (hippocampus, cortex and retina) at both timepoints (Figure 13A, B and C). However, there is a slight tendency for an increase in ChAT levels in the hippocampus at 8 months of age (150.9 ± 23.6% of WT, p=0.0687) (Figure 13A).

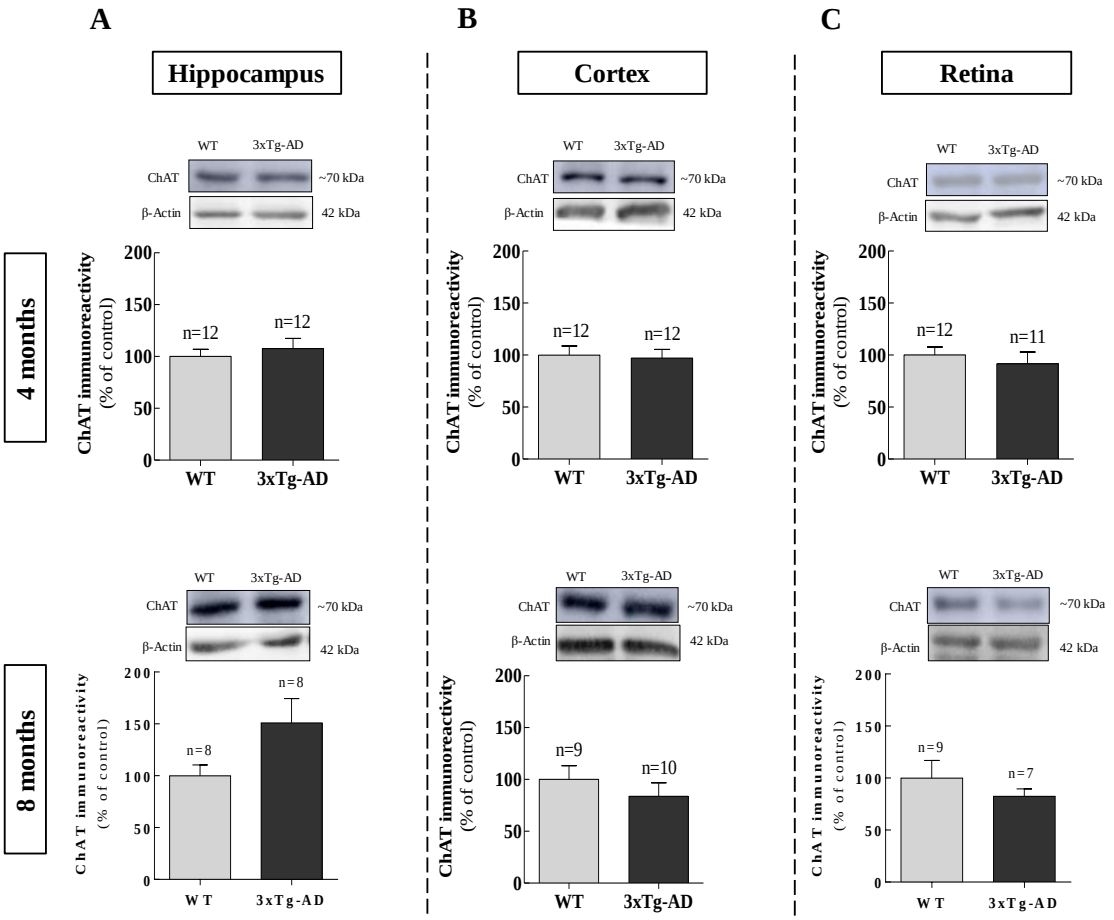

Figure 13 | The protein levels of ChAT remain unchanged in 3xTg-AD mice at 4 and 8 months of age. ChAT protein levels were evaluated in the hippocampal **(A)**, cortical **(B)** and retinal **(C)** homogenates from 3xTg-AD and WT mice at 4 and 8 months old, by Western blotting.
Representative images of protein blots are presented above the respective graph as well as the number of animals used. Results are expressed as mean ± SEM and represent the percentage (%) of WT animals. Statistical significance was assessed by Student's t-test.

4.2.3. No apoptotic cell death was detected in the brain and retina of 3xTg-AD mice at 4 and 8 months of age

Regarding the assessment of apoptotic cell death, no TUNEL positive cells were found in the brain and retina of 3xTg-AD mice, suggesting that at these early timepoints (4 and 8 months) no neuronal loss is present (Figure 14A and B).

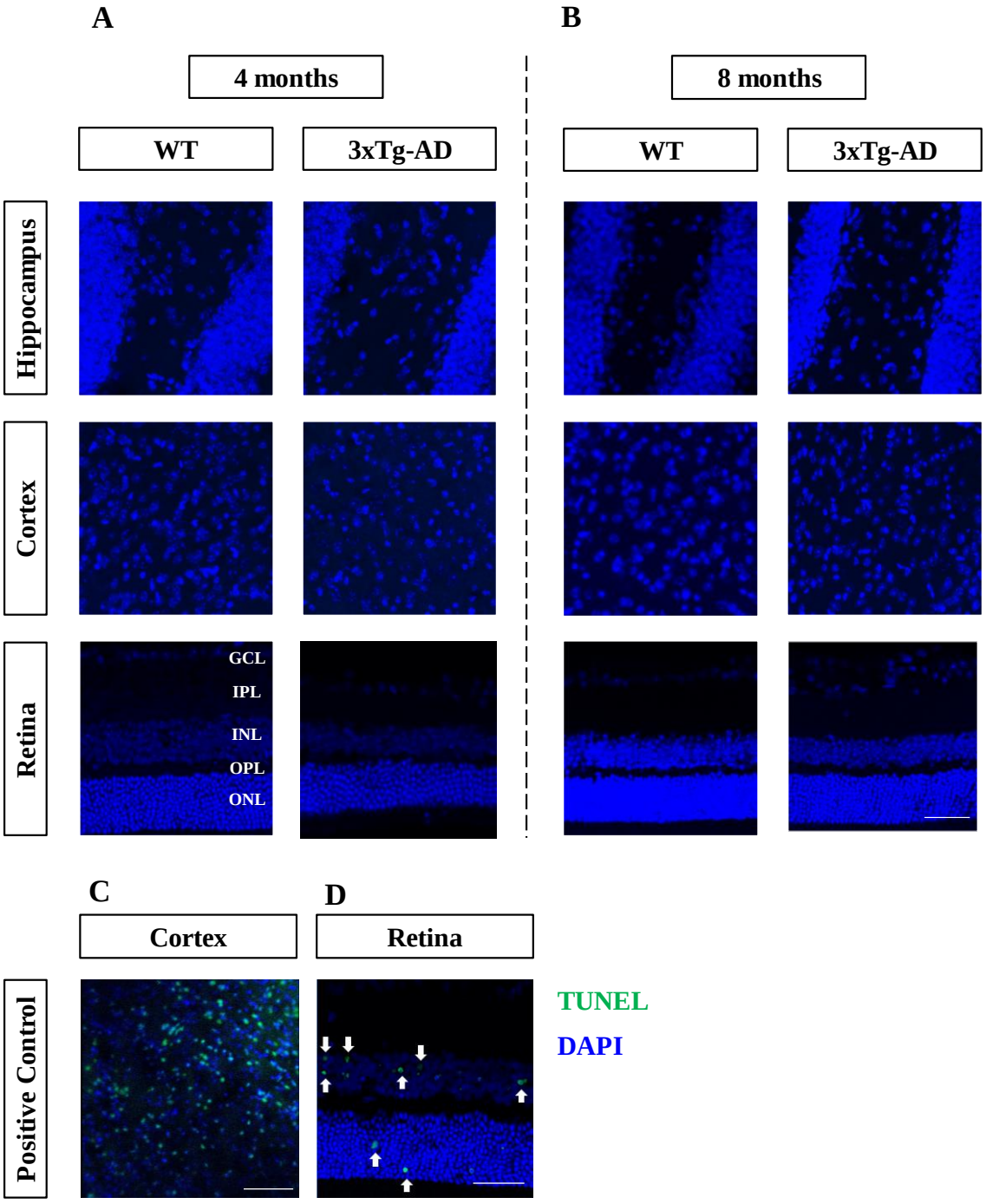

Figure 14 | No apoptotic cell death was detected in the brain and retina of 3xTg-AD mice at 4 and 8 months of age. Apoptotic cell death was evaluated in hippocampal, cortical and retinal sections from 3xTg-AD and WT mice at 4 **(A)** and 8 **(B)** months of age by TUNEL assay. Positive controls (TUNEL-positive cells (green)) of brain **(C)** and retinal **(D)** tissue (sections treated with DNase) are shown. Nuclei were stained with DAPI (blue). Representative images were acquired in the hippocampus (dentate gyrus), cortex and retina. ONL: outer nuclear layer; OPL: outer plexiform layer; INL: inner nuclear layer; IPL: inner plexiform layer; GCL: ganglion cell layer. Scale bar: 50µm.

4.3. Assessment of glial cells reactivity

Neuroinflammation and glial cells reactivity have been reported in AD pathology. In order to analyze if these changes occur early in the brain, and also in the retina, we evaluated the protein content of GFAP (astrocyte marker) in the hippocampus, cortex and retina, and also the levels of vimentin in the retina. Vimentin is an intermediate filament protein highly expressed in Müller cells, glial cells that are present only in the retina. These cells also express GFAP protein in their endfeet. Changes in the expression of these proteins are associated with an increase in their reactivity in response to a stimulus. Immunohistochemistry was performed in retinal cryosections to assess the distribution and reactivity of both astrocytes and Müller cells.

As already mentioned, microglia is another glial cell type, having an important role in the maintenance of homeostasis in both brain and retina. Microglia seek for potential threats, changing its morphology and number when activated, and upregulating the neuroinflammatory environment. Retinal microglia were assessed by immunohistochemistry to check whether there is any difference in microglia number, distribution and reactivity between transgenic and control animals.

4.3.1. GFAP protein levels are altered in the hippocampus and retina of 3xTg-AD mice

In the cortex of 3xTg-AD mice no changes were detected in GFAP protein levels at 4 and 8 months (Figure 15B). However, in the hippocampus, it was detected a significant increase (212.2 ± 27.0 of WT, $p<0.01$) of GFAP protein levels, comparing to WT animals, at 4 months, that did not persist at 8 months (Figure 15A). On the other hand, in the retina, it was detected a significant decrease (43.7 ± 7.0% of WT, $p<0.05$) of GFAP at 8 months (Figure 15C) which was recapitulated by immunohistochemistry Moreover, no changes in the distribution of astrocytes were found between 3xTg-AD and WT mice and between timepoints, being astrocytes almost entirely restricted to the NFL and GCL (Figure 15D).

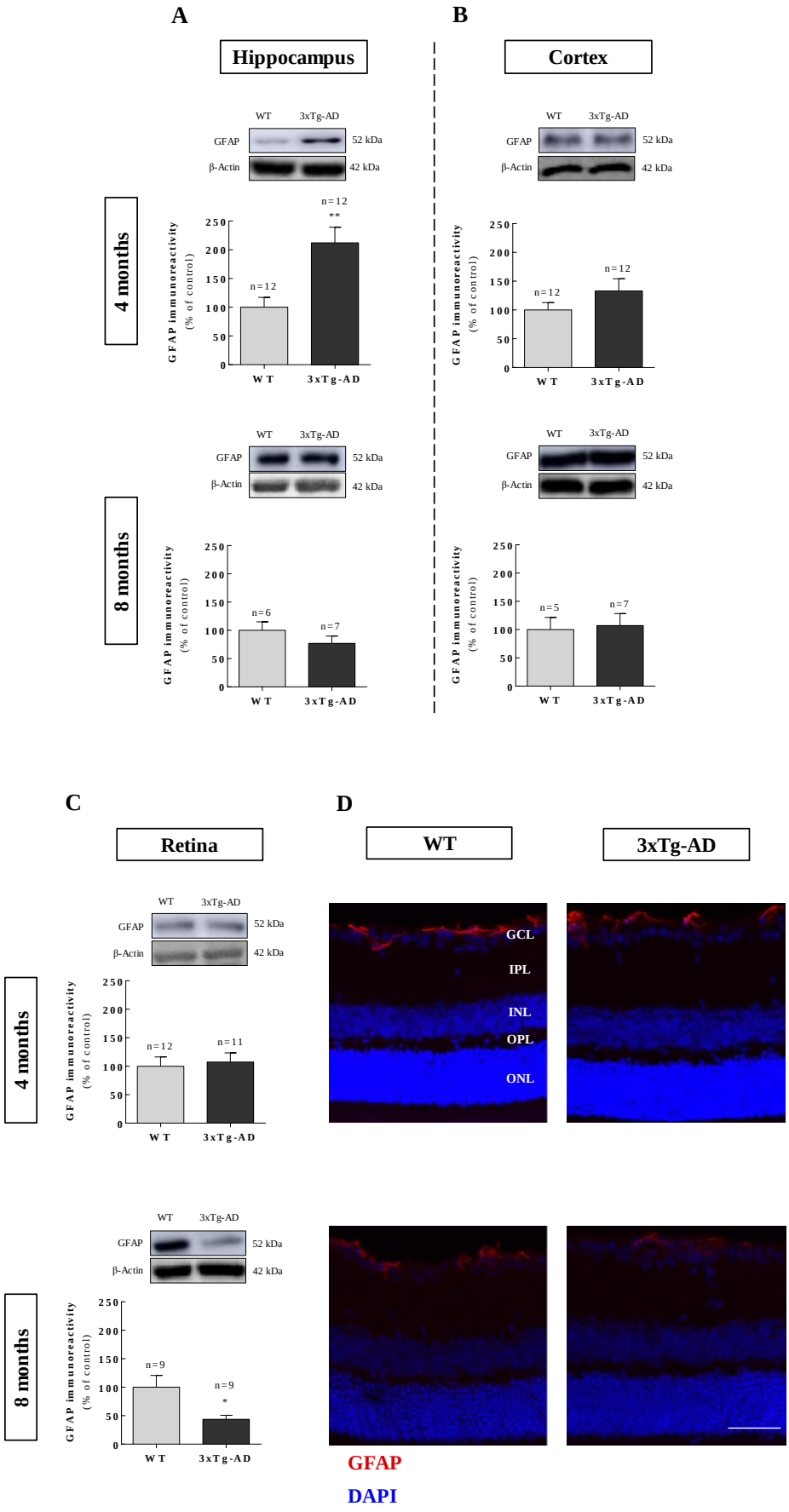
A
Hippocampus
B
Cortex
WT
3xTg-AD
GFAP
52 kDa
β-Actin
42 kDa
4 months
8 months
GFAP immunoreactivity
(% of control)
n=12
n=6
n=7
n=5
**
W T
3xTg-AD
C
Retina
D
WT
3xTg-AD
n=11
n=9
*
GCL
IPL
INL
OPL
ONL
GFAP
DAPI

Figure 15 | The protein levels of GFAP are altered in the hippocampus and retina of 3xTg-AD mice. GFAP protein levels were evaluated in the hippocampal **(A)**, cortical **(B)** and retinal **(C)** homogenates from 3xTg-AD and WT mice at 4 and 8 months old, by Western blotting.
Representative images of protein blots are indicated above the respective graph as well as the number of animals used. Results are expressed as mean ± SEM and represent the percentage (%) of WT animals. Statistical significance was assessed by Student's t-test: *p<0.05, **p<0.01, different from control.
GFAP immunoreactivity (red) was assessed by immunohistochemistry in retinal cryosections from 3xTg-AD and WT mice at 4 and 8 months old using an anti-GFAP antibody **(D)**. Nuclei were stained with DAPI (blue). ONL: outer nuclear layer; OPL: outer plexiform layer; INL: inner nuclear layer; IPL: inner plexiform layer; GCL: ganglion cell layer. Scale bar: 50μm.

4.3.2. No differences detected in retinal Müller cells and microglia of 3xTg-AD mice at 4 and 8 months of age

Vimentin immunoreactivity was assessed by WB and immunohistochemistry. No differences were found in the protein levels and distribution of Müller cells at 4 months (Figure 16A) and 8 months (Figure 16B). They cross the entire thickness of the retina (Figure 16C).

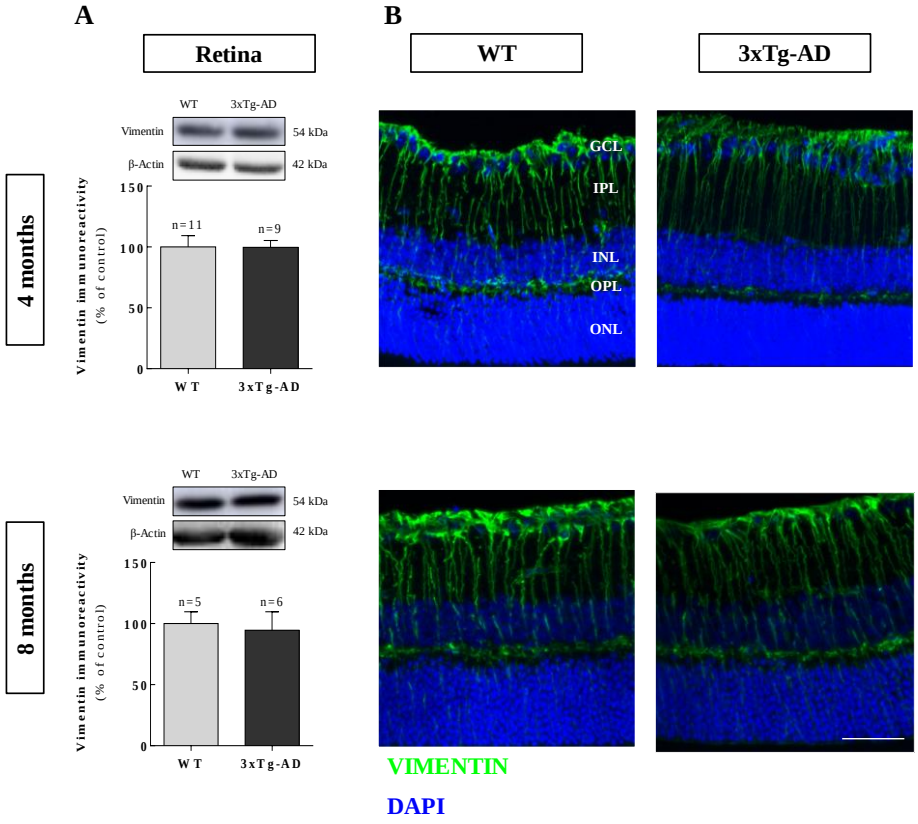

Figure 16 | No differences detected in retinal Müller cells of 3xTg-AD mice at 4 and 8 months of age. Vimentin protein levels were evaluated in retinal homogenates from 3xTg-AD and WT mice at 4 and 8 months old **(A)**, by Western blotting.
Representative images of protein blots are presented above the respective graph as well as the number of animals used. Results are expressed as mean ± SEM and represent the percentage (%) of WT animals. Statistical significance was assessed by Student's t-test.
Vimentin (green) immunoreactivity was assessed by immunohistochemistry in retinal cryosections from 3xTg-AD and WT mice at 4 and 8 months old using an anti-vimentin antibody **(B)**. Nuclei were stained with DAPI (blue). ONL: outer nuclear layer; OPL: outer plexiform layer; INL: inner nuclear layer; IPL: inner plexiform layer; GCL: ganglion cell layer. Scale bar: 50μm.

Under physiological conditions, microglia can be found in the NFL/GCL and within IPL or OPL with processes projecting throughout the synaptic layers of the retina. Microglia reactivity was evaluated in retinal cryosections from 3xTg-AD and control mice by immunohistochemistry using antibodies that recognize the ionized calcium binding adaptor molecule 1 (Iba1), which is a microglia/macrophage-specific calcium-binding protein and the major histocompatibility complex (MHC) class II antigen, which is only expressed by activated microglia and macrophages (OX-6).

No significantly differences were found in the total number of $Iba1^+$ cells or microglia distribution between 3xTg-AD and WT animals at 4 months. Moreover, no activated microglia ($Ox\text{-}6^+$ cells) were found in the retina (Figure 17).

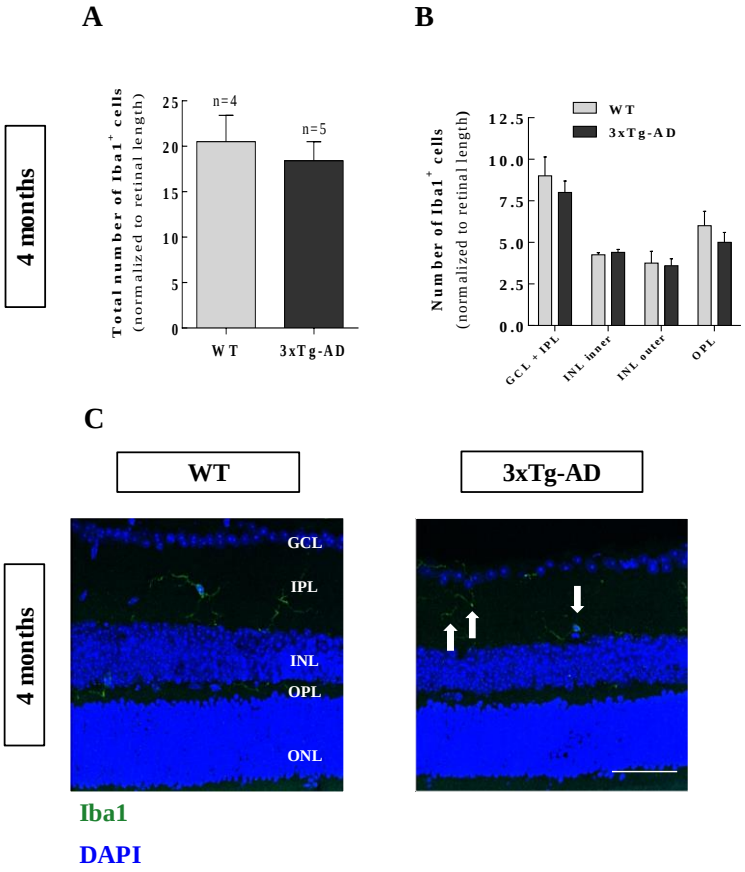

Figure 17 | No differences detected in the number and distribution of retinal microglia in 3xTg-AD mice at 4 months of age. The number and distribution of microglial cells were assessed by immunohistochemistry in retinal cryosections from 3xTg-AD and WT mice 4 months of age. Retinal sections were stained with antibodies against Iba1 (green) and OX-6 (red). Nuclei were stained with DAPI (blue). Iba1$^+$ cells were counted manually. Results represent the mean ± SEM of the number of Iba1$^+$ cells, normalized. Representative images of Iba1 staining are presented. Above each bar it is indicated the number of animals used. Only the right eye was assessed per animal. From each eye, four retinal sections were analyzed. Statistical significance was assessed by Student's t-test. ONL: outer nuclear layer; OPL: outer plexiform layer; INL: inner nuclear layer; IPL: inner plexiform layer; GCL: ganglion cell layer. Scale bar: 50μm.

4.4. Assessment of mitochondrial metabolism

Given that on most parameters presented above no alterations were found in 3xTg-AD mice, comparing with WT animals, at these early timepoints, particularly in the retina, we tried to find subtle molecular changes in mitochondrial metabolism which may be also affected in AD.

Since oxidative stress is intimately associated with mitochondrial dysfunction we assessed the activity of several mitochondrial enzymatic complexes in hippocampal,

cortical and retinal homogenates from 3xTg-AD and WT mice, at 4 and 8 months of age. Firstly, we evaluated the activity of citrate synthase, a marker of mitochondrial mass. Since no significant changes were found in citrate synthase activity in the hippocampus, cortex and retina from 3xTg-AD mice comparing to WT animals, these measures were used as control (Figure 18A, B and C) to adjust the correct value of mitochondrial enzymatic complexes I and IV activities which were also performed by spectrophotometry assays.

Furthermore, we also evaluated the activity of aconitase which is an enzyme from the Krebs cycle responsible for catalyzing the isomerization of citrate to isocitrate. This enzyme is particularly affected by the increase of ROS, which negatively regulates its activity, thereby being an indirect marker of oxidative stress increase.

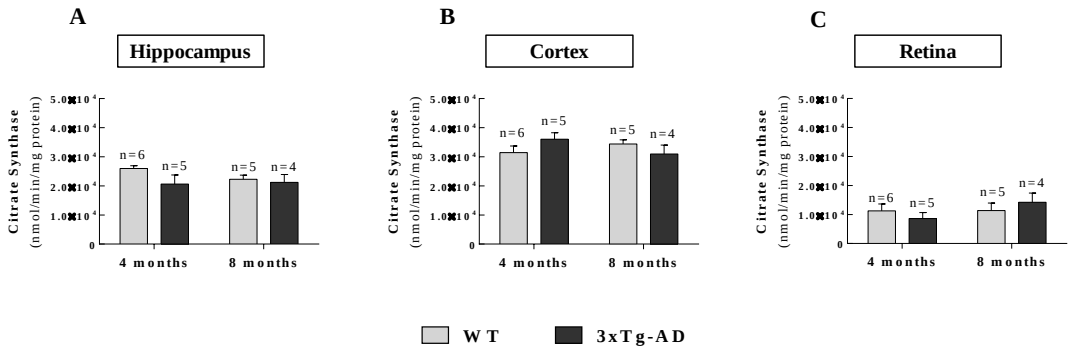

Figure 18 | No alterations in citrate synthase activity in hippocampal, cortical and retinal homogenates at 4 and 8 months. The activity of citrate synthase was measured by spectrophotometry in hippocampal **(A)**, cortical **(B)** and retinal **(C)** homogenates from 3xTg-AD and WT mice at 4 and 8 months old. Above each bar is indicated the number of animals used. Results are presented as nmol of oxaloacetate min^{-1}.mg $protein^{-1}$, as mean ± SEM. Statistical significance was assessed by Kruskal–Wallis ANOVA test followed by Dunn's multiple comparison test.

4.4.1. Increase in the activity of complexes I and IV in the hippocampus and cortex from 3xTg-AD mice at 8 months

Regarding the activity of complex I, there was a significant increase in the hippocampus from 3xTg-AD at 8 months (0.244 ± 0.012, $p<0.05$), comparing to WT animals (0.074 ± 0.005) (Figure 19A). In the cortex from 3xTg-AD mice, we found a decrease in the activity of complex I at 4 months (0.040 ± 0.005, $p<0.01$), comparing to WT animals (0.145 ± 0.018) (Figure 19B). However, at 8 months there was an increase in the activity of complex I, although not significant (0.132 ± 0.030, $p=0.376$)

comparing to WT animals (0.054 ± 0.007) (Figure 19B). Noteworthy, the activity of complex I of WT animals at 8 months decreased (0.054 ± 0.007, $p<0.076$) comparing to animals with 4 months of age (0.145 ± 0.018), although not significant (Figure 19B). Moreover, as shown in Figure 19B, there was a significant increase in the complex I activity in the cortex from 3xTg-AD mice at 8 months (0.132 ± 0.030, $p<0.05$) when compared with 3xTg-AD mice at 4 months (0.040 ± 0.005). On the other hand, in the retina we found a different profile. There are tendencies for a decrease in the complex I activity either between animal groups or between timepoints (Figure 19C).

Regarding the activity of complex IV, there was a significant increase in both hippocampus from 3xTg-AD mice at 8 months (0.076 ± 0.013, $p<0.05$) compared with 3xTg-AD animals at 4 months old (0.032 ± 0.006) as well as in the cortex from 3xTg-AD mice at 8 months (0.090 ± 0.014, $p<0.05$) comparing to 3xTg-AD 4 months old (0.012 ± 0.004). Moreover, although not significant, there were slight increases in the activity of complex IV in the hippocampus and cortex from 3xTg-AD at 8 months old compared with months old WT animals (Figure 19D and E). Again, in the retina, no significant differences were found (Figure 19F).

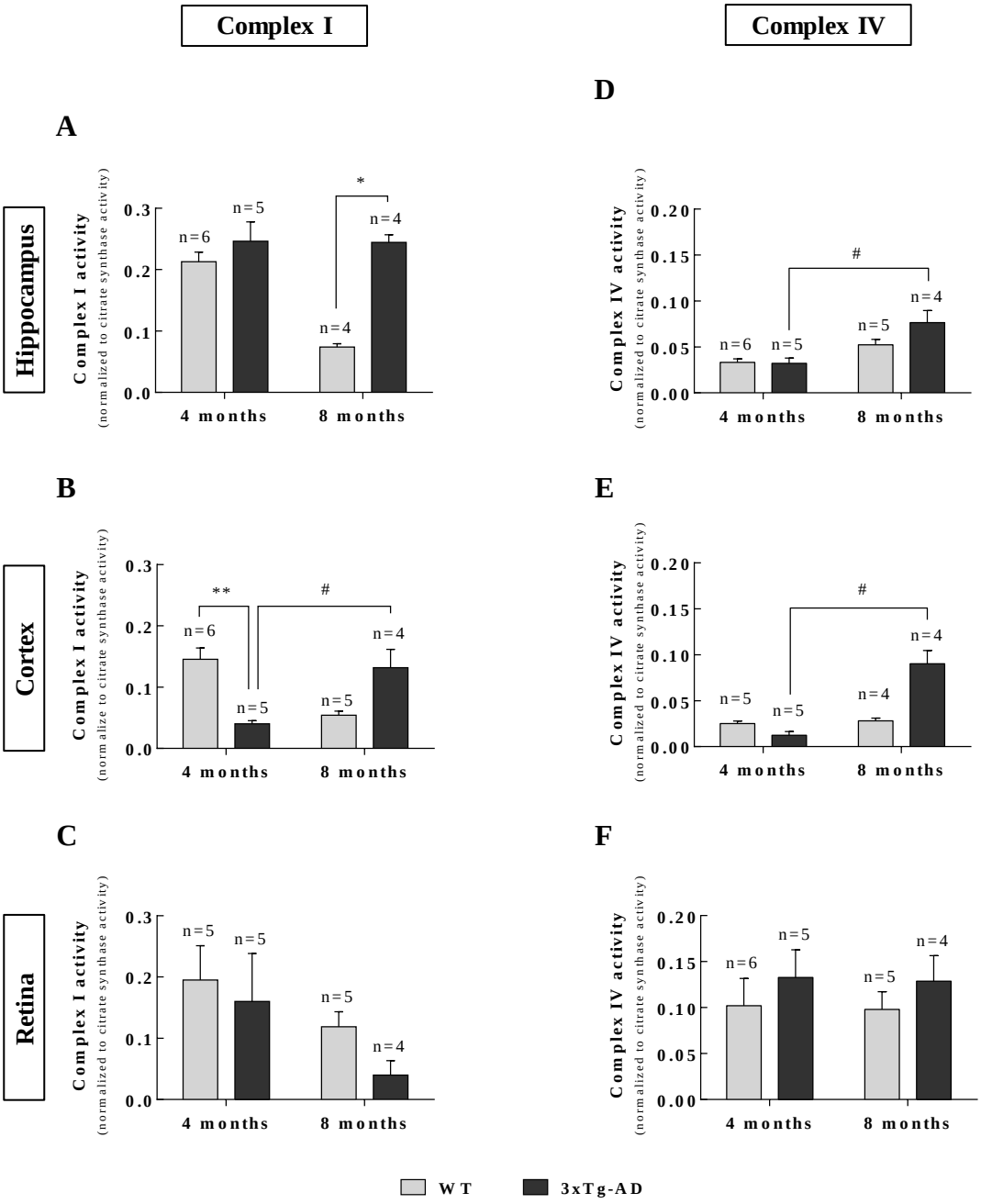

Figure 19 | Increase in the activity of complexes I and IV in the hippocampus and cortex from 3xTg-AD mice at 8 months. The activity of complexes I and IV was measured in hippocampal **(A, D)**, cortical **(B, E)** and retinal **(C, F)** homogenates from 3xTg-AD and WT mice 4 and 8 months old, by spectrophotometry. Above each bar is indicated the number of animals used. Results are presented as a ratio between complexes activity and citrate synthase activity, as mean ± SEM. Statistical significance was assessed by Kruskal–Wallis ANOVA test followed by Dunn's multiple comparison test: *p<0.05; **p<0.01, different from control. #p<0.05, different from 3xTg-AD with 4 months of age.

4.4.2. No significant changes detected in aconitase activity in the brain and retina from 3xTg-AD at 4 and 8 months of age

No significant alterations were found in aconitase activity in the three regions studied. However, at 8 months of age, there was a slight decrease, particularly in the cortex from 3xTg-AD mice (5.920 ± 0.472, p=0.648) comparing to WT animals (8.781 ± 1.234) (Figure 20B) and in the retina from 3xTg-AD mice (6.503 ± 0.952, p=0.095) comparing with WT, (9.789 ± 1.275) (Figure 20C).

In hippocampus, no alterations were detected in the activity of aconitase from 3xTg-AD mice at 4 and 8 months of age (Figure 20A) comparing to WT animals, as well as in the cortex and retina at 4 months of age.

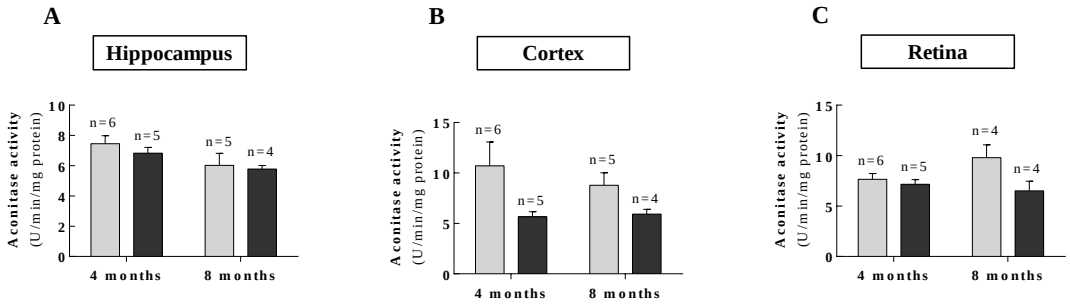

Figure 20 | No significant changes detected in aconitase activity in the brain and retina from 3xTg-AD at 4 and 8 months of age. The activity of aconitase enzyme was measured by spectrophotometry in hippocampal **(A)**, cortical **(B)** and retinal **(C)** homogenates from 3xTg-AD and WT at mice 4 and 8 months old. Above each bar is indicated the number of animals used. Results were presented as $U.min^{-1}.mg\ protein^{-1}$, as mean ± SEM. Statistical significance was assessed by Kruskal–Wallis ANOVA test followed by Dunn's multiple comparison test.

Discussion

6. Discussion

More than one hundred years after being identified, AD became the most common neurodegenerative disorder, affecting almost 47 million people worldwide and still counting, as consequence of a growing elderly population. AD is a multifactorial disorder, having a complex pathophysiology characterized by the presence of Aβ aggregates and neurofibrillary tangles of hyperphosphorylated tau protein, considered the two main hallmarks of AD. They may act synergistically promoting the disease development due to the cascade of events that follows, breaking the neuronal homeostasis. These physiological alterations result in severe cognitive impairments having a huge impact in patient's life. However, so far, AD does not have a cure or efficient treatments to invert this paradigm, possibly because they are applied at too advanced stages when the neuronal loss is irreversible. Therefore, the development of novel and early diagnostic approaches is critical, as well as the improvement of therapeutic tools against disease progression.

Recently, the retina became an interesting research tool to investigate neurodegenerative diseases since it shares the same origin and many similarities with brain and it is also affected during the AD course. When compared with brain, the retina has the advantage of being less complex structurally and easily more accessible to non-invasive exploration. Although there are several imaging techniques able to assess retinal alterations, many gaps remain to be filled before using the retina as an instrument to diagnose early neurodegenerative alterations in the brain.

Having this in mind, we investigated a large set of biological parameters related with changes found in AD brain pathology to clarify whether the retina can be used as a window to detect brain changes and/or if the retina mirrors brain alterations, focusing at early changes. Using the 3xTg-AD mice we assessed the hippocampus, cortex and retina at two early timepoints (4 and 8 months). Although Oddo and colleagues have reported that both male and female 3xTg-AD mice are equally affected, being an advantage that distinguishes this model from others where one gender seems to be more vulnerable, other studies have shown that female 3xTg-AD mice exhibit significantly more aggressive Aβ pathology (Hirata-Fukae *et al*, 2008) and an earlier onset than males (Carroll *et al*, 2007). Given these gender-specific differences in onset and

severity of phenotype, we used solely male 3xTg-AD mice in order to avoid hormonal interference.

In accordance with Oddo and colleagues who created and characterized the 3xTg-AD animal model, which develop an age-related and progressive neuropathological phenotype (Oddo *et al*, 2003), we found an increase in the protein levels of Aβ monomers in the cortex at 4 months of age that increased even more at 8 months suggesting the appearance of amyloid aggregates. Similar results were obtained in the hippocampus. Yet, in the retina, at 4 and 8 months of age, very low concentrations of Aβ were found, with no apparent differences between transgenic mice and control animals neither between timepoints. These results suggest that Aβ amounts in the retina are physiological and no evidence of pathology can be perceived from this result. In fact, previous studies in different models of AD have reported the presence of Aβ monomers as well as amyloid plaques in the retina (Ning *et al*, 2008; Perez *et al*, 2009; Alexandrov *et al*, 2011; Edwards *et al*, 2014), but only at later timepoints. In accordance to our results, Dutescu and colleagues also detected very low levels of Aβ by ELISA (Enzyme-Linked Immunosorbent Assay) in the retinas of APP/PS-1 animal model, demonstrating that retinal Aβ levels were 75 times less than the ones found in transgenic brain. Additionally, no Aβ protein levels were detected by WB, indicating much less Aβ generation in the retina than in the brain tissue (Dutescu *et al*, 2009).

Curiously, previous studies addressing the potential diagnostic value of the retina in AD have mainly focused on Aβ pathology and only a few studies addressed tau protein and its evolution in the pathological context of AD. Schön and colleagues described the first evidence of p-tau in the retina, particularly in the innermost layers, from both AD patients and mice expressing human mutant Tau_{P301S} (Schön *et al*, 2012). Also, Liu and colleagues reported p-tau in the retinas of transgenic mice expressing the APP_{swe} mutation (Tg2576) mice at 14 months of age (Liu *et al*, 2009). Our results show an early increase in p-tau levels at 4 months in the hippocampus, cortex and retina from 3xTg-AD, comparing with age-matched controls. As mentioned before in this thesis, tau protein can be phosphorylated at multiple sites in a very dynamic process in normal conditions. Contrariwise, in AD, tau is abnormally phosphorylated being specific tau phosphorylation sites correlated with the severity of disease (Augustinack *et al*, 2002). We used a specific antibody against a short amino acid sequence containing the

phosphorylated Serine^{396} site of human origin, which has been associated to the earliest events in AD (Mondragón-Rodríguez *et al*, 2014). However, the increase in p-tau protein levels observed at 4 months only persisted in the hippocampus at 8 months, which can be explained by a switch in the phosphorylation sites in the cortex and retina at this timepoint, since in addition to the Serine^{396} site, there are other residues implicated in the early changes of tau phosphorylation, such as Serine^{404} (Otvos *et al*, 1994; Augustinack *et al*, 2002). These findings do not seem to be in line with the Aβ cascade hypothesis associated to this animal model, in which Aβ pathology precedes tau hyperphosphorylation. In fact, Oddo has reported extracellular Aβ deposits in the cortex from 6 months old animals (and even earlier for intracellular Aβ), whereas tau immunoreactivity was only noted within pyramidal neurons of the CA1 subfield at 12 months, before progressing to the neocortex (Oddo *et al*, 2003). However, our findings confirm that both Aβ and p-tau levels are elevated in the 3xTg-AD, at least in the brain.

Despite the comparable overexpression of both tau and APP transgenes in 3xTg-AD, we could detect differences in the three regions in p-tau levels at 4 months, as already mentioned, whereas at the same timepoint no differences were found in APP levels. Yet, in hippocampus, at 8 months, we detected a significant increase in the protein content of APP, which was not replicated in the other tissues. Thus, looking at the increase of Aβ levels in the hippocampus and cortex at 4 and 8 months, the late increase of APP levels suggests that early Aβ accumulation probably resulted due to autophagic impairments, particularly in the degradation of the autophagosome by lysosomes, which are related with the early stages of AD (as reviewed in Correia et al. 2015). In addition, as shown by Tseng and colleagues, Aβ oligomers may impair proteasome activity, contributing even more to Aβ accumulation (Tseng *et al*, 2008). In fact, several theories may explain the increase of Aβ burden, including overexpression and increased metabolism of APP, or a reduction of Aβ clearance, which seems to be the case (Tzekov & Mullan, 2014). According with this idea, BACE protein levels as well as its activity revealed no differences between 3xTg-AD and WT groups in the hippocampus, cortex and retina, at both timepoints, suggesting that the main reason for increased Aβ levels is not the increase of APP processing. Interestingly, these mechanisms may vary at different stages of the disease, so the increase of APP levels detected at 8 months in hippocampus can be the trigger for that switch. However, to

further clarify this issue it would be necessary to evaluate APP levels and BACE activity at later timepoints.

Reports have also shown that deficits in synaptic transmission and LTP (Long Term Potentiation), mainly in the hippocampus, may precede the formation of Aβ plaques and tangles (Oddo *et al*, 2003). Since we did not observe massive alterations in the levels of two synaptic protein (syntaxin and synaptophysin), this suggests that the increases in Aβ peptides and p-tau levels are not sufficient to get extracellular protein deposits in 3xTg-AD model at 4 and 8 months of age. This correlation is supported by Mastrangelo and Bowers who found extracellular Aβ in 3xTg-AD mice only from 15 months onwards (Mastrangelo & Bowers, 2008). However, we cannot exclude that other synaptic proteins such as bassoon, synapsin, PSD95 (postsynaptic density protein 95) or SNAP25 (synaptosomal-associated protein 25) may be changed at the timepoints analyzed. In fact, Carvalho and colleagues reported a decrease in the protein levels of PSD95 and SNAP25 in the hippocampus and cortex from 3xTg-AD at 4 months, whereas synaptophysin is not affected as well (Carvalho et al. 2015). In accordance with the results obtained in the hippocampus and cortex, no differences were found in the retina in syntaxin and synaptophysin protein levels.

Furthermore, we evaluated the levels of ChAT, the enzyme responsible for synthesizing ACh. At 4 and 8 months of age, this protein was not altered in both the hippocampus and cortex as well as in the retina. However, the decrease in ChAT levels or activity is a well-defined feature of AD (White & Ruske, 2002), being the cause or consequence of cholinergic neuronal loss. Although the role of the cholinergic system still remains unclear in the 3xTg-AD model, it was demonstrated that hippocampal and cortical cholinergic neuritic dystrophy increases in an age-dependent manner, as well as a reduction in the number of ChAT-positive cells in the basal forebrain and a decreased in its activity (Perez *et al*, 2011). In the retina, the degeneration of RGCs reported in 14-month-old Tg2576 mice by Williams and collaborators (Williams *et al*, 2013) may have the contribution of cholinergic amacrine cells dysfunction. These cells modulate the signal transmission between bipolar and RGCs. Given that a functional integrated interaction between all retinal cell types is essential for normal vision, some visual problems associated to AD pathology may be due to the impairment on vertical communication among different retinal levels, particularly at the amacrine-RGCs

interaction. Since at the timepoints assessed no changes were observed, it would be interesting to evaluate the relation between amacrine cells, RGCs and cholinergic system.

Apoptotic cell death was also assessed, by TUNEL assay. As expected at these early timepoints, since no alterations in synaptic proteins or ChAT have been found, no signal of neuronal loss was observed in the three regions under study. Curiously, although there are several animal models that mimic the main features of AD, most of them, including the 3xTg-AD model, do not replicate the widespread and devastating loss of neurons observed in the AD brain (Wirths & Bayer, 2010; Zahs & Ashe, 2010).

The subsequent analysis led us to assess the reactivity of glial cells, which plays a critical role in AD progression. When the brain is in a vulnerable state, the first defense line is performed by glial cells in order to reestablish the homeostasis. However, when exposed to chronic inflammation, glial cells drive to an exacerbated response that increase even more the neuroinflammatory environment contributing for the worsening of the disease (Patel *et al*, 2005; Hoeijmakers *et al*, 2016). Yet, our results did not reveal consistent glial changes between timepoints and analyzed regions. Specifically, GFAP protein levels increased in the hippocampus at 4 months and decreased in the retina at 8 months, whereas in the cortex no differences were found. Interestingly, Olabarria and collaborators reported an hypertrophy, specifically in GFAP astrocytes surrounding Aβ plaques, in the hippocampus of the 3xTg-AD model, suggesting differential effects of AD pathology on astrocyte populations depending on their association with Aβ plaques (Olabarria *et al*, 2010). Thus, although presumably there are no Aβ plaques at 4 months in the hippocampus, the increase of GFAP levels at this timepoint may be correlated with increased Aβ levels. Contrariwise, at 8 months, GFAP returns to levels close to the control that may indicate an attempt of the system to preclude the increase of an exaggerated inflammatory response related with disease worsening. According with the evidences in the brain, reports that describe Aβ plaques in the retina demonstrated an interaction between both astrocytes and Müller cells with Aβ in the retinas of 9 month old 3xTg-AD mice, suggesting a complex remodeling similar to astrocyte changes in the AD brain (Edwards *et al*, 2014). However, surprisingly, in the retina we observed an opposite change, comparing to that found in the hippocampus, with a significant decrease of GFAP protein levels at 8 months in 3xTg-AD mice, which is not in

agreement with the brain findings. It is true that we did not detect an increase of Aβ levels in the retina, however we cannot exclude the possibility that the brain, in some way, communicates with the retina in such a way that promotes a retinal response. Given the role of astrocytes in the retina, particularly in constraining retinal vessels to the retina and in maintaining their integrity by supporting endothelial cells that form the blood-retinal barrier (BRB) (Zhang & Stone, 1997), a decrease in the levels of GFAP may represent a decrease in the number of astrocytes as seems to be the case, which may compromise the retinal homeostasis and be one of the factors that lead to visual deficits. Indeed, reports from diabetes field correlate the decrease in GFAP expression in retinal glial cells with the reduction and redistribution of occludin (tight-junction protein) in endothelial cells (Barber *et al*, 2000). Having this in mind, it would be important to evaluate GFAP levels at later timepoints, as well as the brain retinal barrier integrity.

Similarly as recently described by Chidlow and colleagues in the APP/PS-1 animal model, at 3 to 12 months of age (Chidlow *et al*, 2017), no differences were found neither in vimentin protein levels nor in Müller cells reactivity and distribution, at 4 and 8 months. Also, no changes in microglial cell number, distribution and activated phenotype in the retinas of 3xTg-AD mice at 4 months of age were found. Therefore, these results are consistent with the lack of amyloid deposits in the retina as well as the lack of any retinal degeneration at these early timepoints. In general, glial reactivity seems to be a very dynamic process involving different cells, able to change rapidly in response to a stimulus. For that reason, fluctuations mainly in GFAP levels need to be further explored.

Since the majority of the parameters analyzed were not significantly altered at these early timepoints, particularly in the retina, mitochondrial tests were performed trying to assess subtler molecular changes in mitochondrial metabolism, which is also affected in AD (Cardoso *et al*, 2016).

In fact, brain cells, particularly neurons, are highly dependent on mitochondria and small changes in mitochondrial homeostasis may promote a huge impact on neuronal integrity and function (Carvalho et al. 2015). Thus, we took advantage of well-described mitochondrial enzymatic complexes related with AD changes (Rhein et al. 2009; Hauptmann et al. 2009) to assess their activity in the brain and the retina.

Although the differences between groups and timepoints were not the same, in general, we observed an increase of complexes I and IV activity in the brain of 3xTg-AD mice at 8 months of age, which was unexpected, since several reports have shown a decrease in their activities (Carvalho *et al*, 2013). Although the pool of mitochondria is similar between animal groups and timepoints for each tissue, as demonstrated by citrate synthase activity, we cannot discard the hypothesis of increased mitochondrial biogenesis behind this increase of complexes activity, since an increase of mitophagy may also occur. Thus, the pool of mitochondria is maintained although the mitochondrial turnover increases in order to keep mitochondrial properly function. Thereby, we can speculate that at 8 months, a healthier mitochondrial pool in 3xTg-AD may exist, and so, higher enzymatic activity, than in age-matched controls or 3xTg-AD at 4 months (Cardoso *et al*, 2016). In addition, it was demonstrated that Aβ may interfere with these enzymatic complexes compromising their proper function and promoting the increase of ROS formation and the decrease of ATP levels, and so the increase of enzymatic activity may be also explained by an attempt to restore ATP levels (Carvalho et al. 2015). In contrast, the retina revealed a completely different profile, especially in complex I activity, with a tendency to decrease along timepoints. Even though it is not in accordance with brain alterations, the decrease of complex I activity at 8 months in the retina may be also related with ATP deficits caused by oxidative stress, since aconitase activity was slightly decreased, although statistically not significant. Aconitase is a sensitive redox sensor which is inhibited in the presence of ROS, particularly, superoxide ions (Carvalho *et al*, 2013), being an indirect marker of oxidative stress. Although not statistically significant, both cortex and retina presented a decrease in aconitase activity, suggesting an increase of oxidative stress in these regions in 3xTg-AD mice at 8 months.

This group of data adds a note of caution to the expectations that the retina may prove a source of biomarkers for early detection of AD. However, variations may occur not only between different strains of AD transgenic mice, but also between different populations of the same strain which may also explain some of the inconsistent results. A final caveat to our findings relates to the fact that the animal models do not develop AD pathology, they just mimic the pathological phenotype observed in AD patients after a forced mutant genes overexpression.

Final remarks and future perspectives

8. Final remarks and future perspectives

Given the current interest in the potential of the retina as a convenient research tool to study several processes in the CNS, namely those involved in neurodegeneration, our main goal was to investigate the real value of the retina as a window to look into the brain and/or a mirror that may reflect the same alterations that occur in the brain at early timepoints related with AD onset and disease progression. For this purpose, we used the 3xTg-AD mice model, with 4 and 8 months of age, and age-matched WT animals, from which we evaluated several changes in parallel in the hippocampus, cortex and retina.
From the analyses of key molecular players, we conclude that the early accumulation of Aβ peptides in the hippocampus and cortex, but not in the retina, appears to be due to Aβ clearance deficits at these early timepoints.

Regarding the synaptic dysfunction and neuronal loss associated to AD pathology, by evaluating synaptic protein levels and apoptotic cell death, respectively, no changes were detected in 3xTg-AD mice, at 4 and 8 months of age.

Regarding glial cells reactivity, although alterations have been detected in GFAP protein levels in the hippocampus and retina, no changes were found in both microglia and Müller cells, suggesting that in these early timepoints glial cells do not manifest an activated phenotype.

The analysis of mitochondrial metabolism suggests that there is an attempt to maintain a healthy mitochondrial pool and to restore the energy demands in the hippocampus and cortex, at 8 months, whereas in the retina no similar changes were found.

Yet, it is important to emphasize that the timepoints used in this work are very early timepoints, and the assessment was made exclusively on a set of cellular and molecular parameters, which does not necessarily mean that others are not affected as well. Another important issue refers to each experimental technique used and its specific detection limit, which may influence the outcome, regarding whether there are differences or not. Nevertheless, to complement this work and given that just a few changes have been detected in the early timepoints, it would be interesting to evaluate more subtle changes and obviously to assess later timepoints.

Specifically, given the central roles of Aβ and phosphorylated tau protein as biomarkers of AD pathophysiology, it would be interesting to assess even earlier

timepoints that would allow us to know more precisely when the first changes in the accumulation of these two proteins start appearing in both hippocampus and cortex and correlate them with the differences observed at the level of mitochondrial dysfunction and glial reactivity, namely the astrocytes, since they were the only significant alterations found in 3xTg-AD at 4 months of age. Moreover, the assessment of ATP and ROS levels in the brain and retina would give a better idea regarding the mitochondrial impairments that may be one of the most important early changes in AD pathology. Additionally, the close communication between brain and retina, in such a way that may induce retinal changes, even without the presence of the main hallmarks of AD pathology, is an interesting hypothesis to further explore.

In addition, given the evidence supporting the degeneration of RGCs in transgenic mice, the analysis of these cells, as well as amacrine cells, could give us a better insight about retinal deficits associated to AD. Given the cholinergic system impairment in AD pathology, although no differences in ChAT protein levels have been found, its activity may be compromised, thus having a role, although indirectly, with RGCs degeneration.

Regarding the role of the glial cells in both brain and retina in AD, it would be interesting to try to identify more subtle changes related with glial cells morphology, namely the number and length of their processes in both microglia and astrocytes. Indeed, Davies and colleagues have reported changes in microglia morphology and a reduction in their arborization in human AD brain (Davies et al. 2016). Finally, the increase of glial reactivity and the consequent increase of pro-inflammatory cytokines is also an important issue to be addressed in both retina and brain.

Thus, based on the results presented, we can conclude that the retina, at least at these early timepoints, does not mirror the changes found in the brain, particularly the one considered the main hallmark of the disease, which is the Aβ accumulation. Although many of the analyzed parameters are not changed in the regions studied, increased Aβ levels are not as evident in the retina as in the brain from 3xTg-AD mice. Since it is well described that the accumulation of Aβ is one of the main causative agents for AD progression, this issue limits the potential of the retina, as a mirror of the brain, particularly in this animal model. Nevertheless, the increase of phosphorylated

tau protein in the retina at 4 months in 3xTg-AD mice indicates that the retina seems to be also affected in this animal model, however with less severity.

Taking this into account, this work does not support the hypothesis that detectable retinal pathology occurs in the same line and, with similar profile as in the brain, thereby not being a reliable mirror of brain alterations in AD, particularly for the early timepoints.

References

7. References

Alexandrov PN, Pogue A, Bhattacharjee S & Lukiw WJ (2011) Retinal amyloid peptides and complement factor H in transgenic models of Alzheimer's disease. *Neuroreport* **22:** 623–627

Alzheimer's Disease International (AZ) (2015) World Alzheimer Report 2015. London, UK. *Alzheimer's Dis. Int.*

Alzheimer A (1907) Uber eine eigenartige Erkrankung der Hirnrinde. *Allg Zeits Psychiatry Psych. Y Gerichtl. Med* **64:** 146–8

Augustinack JC, Schneider A, Mandelkow EM & Hyman BT (2002) Specific tau phosphorylation sites correlate with severity of neuronal cytopathology in Alzheimer's disease. *Acta Neuropathol.* **103:** 26–35

Barber AJ, Antonetti DA & Gardner TW (2000) Altered Expression of Retinal Occludin and Glial Fibrillary Acidic Protein in Experimental Diabetes. *Investig. Ophthalmol. Vis. Sci.* **41:** 3561–3568

Bateman RJ, Xiong C, Benzinger TLS, Fagan AM, Goate A, Fox NC, Marcus DS, Cairns NJ, Xie X, Blazey TM, Holtzman DM, Santacruz A, Buckles V, Oliver A, Moulder K, Aisen PS, Ghetti B, Klunk WE, McDade E, Martins RN, et al (2012) Clinical and Biomarker Changes in Dominantly Inherited Alzheimer's Disease. *N. Engl. J. Med.* **367:** 795–804

Bilkei-Gorzo A (2014) Genetic mouse models of brain ageing and Alzheimer's disease. *Pharmacol. Ther.* **142:** 244–257

Bolmont T, Haiss F, Eicke D, Radde R, Mathis CA, Klunk WE, Kohsaka S, Jucker M & Calhoun ME (2008) Dynamics of the Microglial/Amyloid Interaction Indicate a Role in Plaque Maintenance. *J. Neurosci.* **28:** 4283–4292

Braak H & Braak E (1991) Neuropathological stageing of Alzheimer-related changes. *Acta Neuropathol.* **82:** 239–259

Braak H & Braak E (1998) Evolution of neuronal changes in the course of Alzheimer's disease. *J. Neural Transm. Suppl.* **53:** 127–40

Brautigan BDL, Ferguson-miller S & Margoliash E (1978) Mitochondrial cytochrome c: preparation and activity of native and chemically modified cytochromes c. **:** 128–164

Brion JP, Hanger DP, Bruce MT, Couck AM, Flament-Durand J & Anderton BH

(1991) Tau in Alzheimer neurofibrillary tangles. N- and C-terminal regions are differentially associated with paired helical filaments and the location of a putative abnormal phosphorylation site. *Biochem J* **273(Pt 1):** 127–133

Brion JP, Smith C, Couck AM, Gallo JM & Anderton BH (1993) Developmental changes in tau phosphorylation: fetal tau is transiently phosphorylated in a manner similar to paired helical filament-tau characteristic of Alzheimer's disease. *J. Neurochem.* **61:** 2071–80

Cardoso S, Carvalho C, Correia SC, Sei??a RM & Moreira PI (2016) Alzheimer's Disease: From Mitochondrial Perturbations to Mitochondrial Medicine. *Brain Pathol.* **26:** 632–647

Carroll JC, Rosario ER, Chang L, Stanczyk FZ, Oddo S, LaFerla FM & Pike CJ (2007) Progesterone and Estrogen Regulate Alzheimer-Like Neuropathology in Female 3xTg-AD Mice. *J. Neurosci.* **27:** 13357–13365

Carvalho C, Correia SC, Cardoso S, Plácido AI, Candeias E, Duarte AI & Moreira PI (2015a) The role of mitochondrial disturbances in Alzheimer, Parkinson and Huntington diseases. *Expert Rev. Neurother.* **15:** 867–84

Carvalho C, Machado N, Mota PC, Correia SC, Cardoso S, Santos RX, Santos MS, Oliveira CR & Moreira PI (2013) Type 2 diabetic and Alzheimer's disease mice present similar behavioral, cognitive, and vascular anomalies. *J.Alzheimers.Dis.* **35:** 623–635

Carvalho C, Santos MS, Oliveira CR & Moreira PI (2015b) Alzheimer's disease and type 2 diabetes-related alterations in brain mitochondria, autophagy and synaptic markers. *Biochim. Biophys. Acta - Mol. Basis Dis.* **1852:** 1665–1675

Caspersen C (2005) Mitochondrial A : a potential focal point for neuronal metabolic dysfunction in Alzheimer's disease. *FASEB J.*

Castellano JM, Kim J, Stewart FR, Jiang H, DeMattos RB, Patterson BW, Fagan AM, Morris JC, Mawuenyega KG, Cruchaga C, Goate AM, Bales KR, Paul SM, Bateman RJ & Holtzman DM (2011) Human apoE Isoforms Differentially Regulate Brain Amyloid- Peptide Clearance. *Sci. Transl. Med.* **3:** 89ra57-89ra57

Chami L & Checler F (2012) BACE1 is at the crossroad of a toxic vicious cycle involving cellular stress and β-amyloid production in Alzheimer's disease. *Mol. Neurodegener.* **7:** 52

Chang LYL, Lowe J, Ardiles A, Lim J, Grey AC, Robertson K, Danesh-Meyer H, Palacios AG & Acosta ML (2014) Alzheimer's disease in the human eye. Clinical tests that identify ocular and visual information processing deficit as biomarkers. *Alzheimer's Dement.* **10:** 251–261

Chasseigneaux S & Allinquant B (2012) Functions of Aβ, sAPPα and sAPPβ: Similarities and differences. *J. Neurochem.* **120:** 99–108

Chen Y & Dong C (2009) Abeta40 promotes neuronal cell fate in neural progenitor cells. *Cell Death Differ* **16:** 386–394

Cheung CY, Ong YT, Hilal S, Ikram MK, Low S, Ong YL, Venketasubramanian N, Yap P, Seow D, Chen CL WT (2015) Retinal ganglion cell analysis using high-definition optical coherence tomography in patients with mild cognitive impairment and alzheimer's disease. *J. Alzheimer's Dis.* **45:** 45–56

Chidlow G, Wood JPM, Manavis J, Finnie J & Casson RJ (2017) Investigations into Retinal Pathology in the Early Stages of a Mouse Model of Alzheimer's Disease. *J. Alzheimer's Dis.* **56:** 655–675

Chou JL, Shenoy D V, Thomas N, Choudhary PK, Laferla FM, Goodman SR & Breen GA (2011) Early dysregulation of the mitochondrial proteome in a mouse model of Alzheimer's disease. *J Proteomics* **74:** 466–479

Conejero-Goldberg C, Gomar JJ, Bobes-Bascaran T, Hyde TM, Kleinman JE, Herman MM, Chen S, Davies P & Goldberg TE (2014) APOE2 enhances neuroprotection against Alzheimer's disease through multiple molecular mechanisms. *Mol. Psychiatry* **19:** 1243–1250

Coore HG, Denton RM, Martin BR & Randle PJ (1971) Regulation of adipose tissue pyruvate dehydrogenase by insulin and other hormones. *Biochem. J.* **125:** 115–127

Correia SC, Resende R, Moreira PI & Pereira CM (2015) Alzheimer's Disease-Related Misfolded Proteins and Dysfunctional Organelles on Autophagy Menu. *DNA Cell Biol.* **34:** 261–273

Counts SE, Ikonomovic MD, Mercado N, Vega IE & Mufson EJ (2017) Biomarkers for the Early Detection and Progression of Alzheimer's Disease. *Neurotherapeutics* **14:** 35–53

De-paula VJ, Radanovic M, Diniz BS & Forlenza O V (2012) Protein Aggregation and Fibrillogenesis in Cerebral and Systemic Amyloid Disease. **65:** Chapter 14

Dinet V, Bruban J, Chalour N, Maoui A, An N, Jonet L, Buret A, Behar-Cohen F, Klein C, Tréton J & Mascarelli F (2012) Distinct effects of inflammation on gliosis, osmohomeostasis, and vascular integrity during amyloid beta-induced retinal degeneration. *Aging Cell* **11:** 683–693

Drechsel DN, Hyman a a, Cobb MH & Kirschner MW (1992) Modulation of the dynamic instability of tubulin assembly by the microtubule-associated protein tau. *Mol. Biol. Cell* **3:** 1141–54

Dutescu RM, Li Q-X, Crowston J, Masters CL, Baird PN & Culvenor JG (2009) Amyloid precursor protein processing and retinal pathology in mouse models of Alzheimer's disease. *Graefes Arch. Clin. Exp. Ophthalmol.* **247:** 1213–21

Edwards MM, Rodríguez JJ, Gutierrez-Lanza R, Yates J, Verkhratsky A & Lutty GA (2014) Retinal macroglia changes in a triple transgenic mouse model of Alzheimer's disease. *Exp. Eye Res.* **127:** 252–260

Farrer LA, Cupples LA, Haines JL, Hyman B, Kukull W a, Mayeux R, Myers RH, Pericak-Vance MA, Risch N & van Duijn CM (1997) Effects of age, sex, and ethnicity on the association between apolipoprotein E genotype and Alzheimer disease. A meta-analysis. APOE and Alzheimer Disease Meta Analysis Consortium. *JAMA* **278:** 1349–1356

Giri M, Zhang M LY (2016) Genes associated with Alzheimer's disease: an overview and current status. *Clin. Interv. Aging* **11:** 665—681

Glenner GG & Wong CW (1984) Alzheimer's disease: initial report of the purification and characterization of a novel cerebrovascular amyloid protein. *Biochem. Biophys. Res. Commun.* **120:** 885–890

Goate A, Chartier-Harlin M & Mullan M (1991) Segregation of a missense mutation in the amyloid precursor protein gene with familial Alzheimer's disease. *Nature* **349:** 704–706

Goedert M, Jakes R, Crowther R a, Six J, Lübke U, Vandermeeren M, Cras P, Trojanowski JQ & Lee VM (1993) The abnormal phosphorylation of tau protein at Ser-202 in Alzheimer disease recapitulates phosphorylation during development. *Proc. Natl. Acad. Sci. U. S. A.* **90:** 5066–5070

Grundke-Iqbal I, Iqbal K, Tung YC, Quinlan M, Wisniewski HM & Binder LI (1986) Abnormal phosphorylation of the microtubule-associated protein tau (tau) in

Alzheimer cytoskeletal pathology. *Proc. Natl. Acad. Sci.* **83:** 4913–4917

Gupta VK, Chitranshi N, Gupta VB, Golzan M, Dheer Y, Wall R V, Georgevsky D, King AE, Vickers JC, Chung R & Graham S (2016) Amyloid beta accumulation and inner retinal degenerative changes in Alzheimer's disease transgenic mouse. *Neurosci Lett* **623:** 52–56

Haass C & Selkoe DJ (1993) Cellular processing of β-amyloid precursor protein and the genesis of amyloid β-peptide. *Cell* **75:** 1039–1042

Hamer M & Chida Y (2009) Physical activity and risk of neurodegenerative disease: a systematic review of prospective evidence. *Psychol. Med.* **39:** 3

Hart NJ, Koronyo Y, Black KL & Koronyo-Hamaoui M (2016) Ocular indicators of Alzheimer???s: exploring disease in the retina. *Acta Neuropathol.* **132:** 767–787

Hauptmann S, Scherping I, Dröse S, Brandt U, Schulz KL, Jendrach M, Leuner K, Eckert A & Müller WE (2009) Mitochondrial dysfunction: An early event in Alzheimer pathology accumulates with age in AD transgenic mice. *Neurobiol. Aging* **30:** 1574–1586

Heneka MT, Carson MJ, Khoury J El, Landreth GE, Brosseron F, Feinstein DL, Jacobs AH, Wyss-Coray T, Vitorica J, Ransohoff RM, Herrup K, Frautschy SA, Finsen B, Brown GC, Verkhratsky A, Yamanaka K, Koistinaho J, Latz E, Halle A, Petzold GC, et al (2015) Neuroinflammation in Alzheimer's disease. *Lancet Neurol.* **14:** 388–405

Hinton DR, Sadun AA, Blanks JC & Miller CA (1986) Optic-Nerve Degeneration in Alzheimer's Disease. *N. Engl. J. Med.* **315:** 485–487

Hirata-Fukae C, Li HF, Hoe HS, Gray AJ, Minami SS, Hamada K, Niikura T, Hua F, Tsukagoshi-Nagai H, Horikoshi-Sakuraba Y, Mughal M, Rebeck GW, LaFerla FM, Mattson MP, Iwata N, Saido TC, Klein WL, Duff KE, Aisen PS & Matsuoka Y (2008) Females exhibit more extensive amyloid, but not tau, pathology in an Alzheimer transgenic model. *Brain Res.* **1216:** 92–103

Ho CY, Troncoso JC, Knox D, Stark W EC (2014) Beta-amyloid, phospho-tau and alpha-synuclein deposits similar to those in the brain are not identified in the eyes of Alzheimer's and Parkinson's disease patients. *Brain Pathol.*

Hoeijmakers L, Heinen Y, van Dam A-M, Lucassen PJ & Korosi A (2016) Microglial Priming and Alzheimer's Disease: A Possible Role for (Early) Immune Challenges

and Epigenetics? *Front. Hum. Neurosci.* **10:**

Holtzman DM, Morris JC & Goate AM (2011) Alzheimer's Disease: The Challenge of the Second Century. *Sci. Transl. Med.* **3:** 77sr1-77sr1

Huang YWA, Zhou B, Wernig M & S??dhof TC (2017) ApoE2, ApoE3, and ApoE4 Differentially Stimulate APP Transcription and A?? Secretion. *Cell* **168:** 427–441.e21

Imtiaz B, Tolppanen A-M, Kivipelto M & Soininen H (2014) Future directions in Alzheimer's disease from risk factors to prevention. *Biochem. Pharmacol.* **88:** 661–670

Iqbal K, Del C. Alonso A, Chen S, Chohan MO, El-Akkad E, Gong CX, Khatoon S, Li B, Liu F, Rahman A, Tanimukai H & Grundke-Iqbal I (2005) Tau pathology in Alzheimer disease and other tauopathies. *Biochim. Biophys. Acta - Mol. Basis Dis.* **1739:** 198–210

Itagaki S, McGeer PL, Akiyama H, Zhu S & Selkoe D (1989) Relationship of microglia and astrocytes to amyloid deposits of Alzheimer disease. *J. Neuroimmunol.* **24:** 173–182

Ittner LM & Götz J (2011) Amyloid-β and tau — a toxic pas de deux in Alzheimer's disease. *Nat. Rev. Neurosci.* **12:** 65–72

Jack CR, Knopman DS, Jagust WJ, Shaw LM, Aisen PS, Weiner MW, Petersen RC & Trojanowski JQ (2010) Hypothetical model of dynamic biomarkers of the Alzheimer's pathological cascade. *Lancet Neurol.* **9:** 119–128

Johnson G V & Stoothoff WH (2004) Tau phosphorylation in neuronal cell function and dysfunction. *J. Cell Sci.* **117:** 5721–5729

Justino L, Kergoat MJ, Bergman H, Chertkow H, Robillard A & Kergoat H (2001) Neuroretinal function is normal in early dementia of the Alzheimer type. *Neurobiol. Aging* **22:** 691–695

Kang J, Lemaire H-G, Unterbeck A, Salbaum J, Masters C, Grzeschik K-H, Multhaup G, Beyreuther K & M??ller-Hill B (1987) The precursor of Alzheimer??s disease amyloid A4 protein resembles a cell-surface receptor. *Alzheimer Dis. Assoc. Disord.* **1:** 206–207

Kar S, Slowikowski SPM, Westaway D & Mount HTJ (2004) Interactions between β-amyloid and central cholinergic neurons : implications for Alzheimer ' s disease. *J.*

Psychiatry Neurosci. **29:** 427–442

Kergoat H, Kergoat MJ, Justino L, Chertkow H, Robillard a & Bergman H (2001) An evaluation of the retinal nerve fiber layer thickness by scanning laser polarimetry in individuals with dementia of the Alzheimer type. *Acta Ophthalmol. Scand.* **79:** 187–91

Kettenmann H, Hanisch U-K, Noda M & Verkhratsky A (2011) Physiology of Microglia. *Physiol. Rev.* **91:** 461–553

Kolb H (2001) Glial Cells of the Retina. *Webvision Organ. Retin. Vis. Syst.***:** 1–11

Koronyo-Hamaoui M, Koronyo Y, Ljubimov A V., Miller CA, Ko MHK, Black KL, Schwartz M & Farkas DL (2011) Identification of amyloid plaques in retinas from Alzheimer's patients and noninvasive in vivo optical imaging of retinal plaques in a mouse model. *Neuroimage* **54:**

Krebs HA & Holzach O (1952) The conversion of citrate into cis-aconitate and isocitrate in the presence of aconitase. *Biochem. J.* **52:** 527–8

Lazarov O, Robinson J, Tang Y-P, Hairston IS, Korade-Mirnics Z, Lee VM-Y, Hersh LB, Sapolsky RM, Mirnics K & Sisodia SS (2005) Environmental Enrichment Reduces A[beta] Levels and Amyloid Deposition in Transgenic Mice. *Cell* **120:** 701–713

Levy-Lahad E, Wasco W, Poorkaj P, Romano DM, Oshima J, Pettingell WH, Yu CE, Jondro PD, Schmidt SD, Wang K & et al. (1995) Candidate gene for the chromosome 1 familial Alzheimer's disease locus. *Science (80-.).* **269:** 973–977

Lim JKH, Li QX, He Z, Vingrys AJ, Wong VHY, Currier N, Mullen J, Bui B V. & Nguyen CTO (2016) The eye as a biomarker for Alzheimer's disease. *Front. Neurosci.* **10:** 1–14

Lindwall G & Cole RD (1984) Phosphorylation affects the ability of tau protein to promote microtubule assembly. *J. Biol. Chem.* **259:** 5301–5305

Liu B, Rasool S, Yang Z, Glabe CG, Schreiber SS, Ge J & Tan Z (2009) Amyloid-Peptide Vaccinations Reduce β-Amyloid Plaques but Exacerbate Vascular Deposition and Inflammation in the Retina of Alzheimer's Transgenic Mice. *Am. J. Pathol.* **175:** 2099–2110

Liu C-C, Kanekiyo T, Xu H & Bu G (2013) Apolipoprotein E and Alzheimer disease: risk, mechanisms and therapy. *Nat. Rev. Neurol.* **9:** 106–118

London A, Benhar I & Schwartz M (2012) The retina as a window to the brain—from eye research to CNS disorders. *Nat. Rev. Neurol.* **9:** 44–53

Long J, Ma J, Luo C, Mo X, Sun L, Zang W & Liu J (2009) Comparison of two methods for assaying complex I activity in mitochondria isolated from rat liver, brain and heart. *Life Sci* **85:** 276–280

Lu Y, Li Z, Zhang X, Ming B, Jia J, Wang R & Ma D (2010) Retinal nerve fiber layer structure abnormalities in early Alzheimer's disease: Evidence in optical coherence tomography. *Neurosci. Lett.* **480:** 69–72

Lustbader JW (2004) ABAD Directly Links A to Mitochondrial Toxicity in Alzheimer's Disease. *Science (80-.).* **304:** 448–452

Madeira MH, Ambrósio AF & Santiago AR (2015a) Glia-mediated retinal neuroinflammation as a biomarker in Alzheimer's disease. *Ophthalmic Res.* **54:** 204–211

Madeira MH, Boia R, Santos PF, Ambrósio AF & Santiago AR (2015b) Contribution of microglia-mediated neuroinflammation to retinal degenerative diseases. *Mediators Inflamm.* **2015:**

Manczak M, Park BS, Jung Y & Reddy PH (2004) Differential expression of oxidative phosphorylation genes in patients with Alzheimer's disease: implications for early mitochondrial dysfunction and oxidative damage. *Neuromolecular Med.* **5:** 147–162

Masters CL, Bateman R, Blennow K, Rowe CC, Sperling RA & Cummings JL (2015) Alzheimer's disease. *Nat. Rev. Dis. Prim.* **1:** 15056

Mastrangelo M a & Bowers WJ (2008) Detailed immunohistochemical characterization of temporal and spatial progression of Alzheimer's disease-related pathologies in male triple-transgenic mice. *BMC Neurosci.* **9:** 81

Mondragón-Rodríguez S, Perry G, Luna-Muñoz J, Acevedo-Aquino MC & Williams S (2014) Phosphorylation of tau protein at sites Ser396-404 is one of the earliest events in Alzheimer's disease and Down syndrome. *Neuropathol. Appl. Neurobiol.* **40:** 121–135

Morris RGR, Anderson E, Lynch GSG, Baudry M, Anderson A & Baudry B (1986) Selective impairment of learning and blockade of long-term potentiation by an iV-methyl-D-aspartate receptor antagonist, AP5. *Nature* **319:** 774–776

Nath S, Agholme L, Kurudenkandy FR, Granseth B, Marcusson J & Hallbeck M (2012) Spreading of Neurodegenerative Pathology via Neuron-to-Neuron Transmission of -Amyloid. *J. Neurosci.* **32:** 8767–8777

Ning A, Cui J, To E, Ashe KH & Matsubara J (2008) Amyloid-beta deposits lead to retinal degeneration in a mouse model of Alzheimer disease. *Invest. Ophthalmol. Vis. Sci.* **49:** 5136–5143

O'Brien RJ & Wong PC (2011) Amyloid Precursor Protein Processing and Alzheimer's Disease. *Annu. Rev. Neurosci.* **34:** 185–204

Oddo S, Caccamo A, Shepherd JD, Murphy MP, Golde TE, Kayed R, Metherate R, Mattson MP, Akbari Y & LaFerla FM (2003) Triple-Transgenic Model of Alzheimer's Disease with Plaques and TanglesIntracellular Aβ and Synaptic Dysfunction. *Neuron* **39:** 409–421

Oddo S, Caccamo A, Smith IF, Green KN & LaFerla FM (2006) A Dynamic Relationship between Intracellular and Extracellular Pools of Aβ. *Am. J. Pathol.* **168:** 184–194

Olabarria M, Noristani HN, Verkhratsky A & Rodríguez JJ (2010) Concomitant astroglial atrophy and astrogliosis in a triple transgenic animal model of Alzheimer's disease. *Glia* **58:** 831–838

Otvos L, Feiner L, Lang E, Szendrei GI, Goedert M & Lee VM (1994) Monoclonal antibody PHF-1 recognizes tau protein phosphorylated at serine residues 396 and 404. *J. Neurosci. Res.* **39:** 669–673

Padurariu M, Ciobica A, Mavroudis I, Fotiou D & Baloyannis S (2012) Hippocampal neuronal loss in the CA1 and CA3 areas of Alzheimer's disease patients. *Psychiatr. Danub.* **24:** 152–158

Palmer AM (2011) Neuroprotective therapeutics for Alzheimers disease: Progress and prospects. *Trends Pharmacol. Sci.* **32:** 141–147

Paquet C, Boissonnot M, Roger F, Dighiero P, Gil R & Hugon J (2007) Abnormal retinal thickness in patients with mild cognitive impairment and Alzheimer's disease. *Neurosci. Lett.* **420:** 97–99

Parisi V, Restuccia R, Fattapposta F, Mina C, Bucci MG & Pierelli F (2001) Morphological and functional retinal impairment in Alzheimer's disease patients. *Clin. Neurophysiol.* **112:** 1860–1867

Patel NS, Paris D, Mathura V, Quadros AN, Crawford FC & Mullan MJ (2005) Inflammatory cytokine levels correlate with amyloid load in transgenic mouse models of Alzheimer's disease. *J. Neuroinflammation* **2:** 9

Paxinos G, Franklin KBJ, Paxinos, G and Franklin KBJ, Paxinos G & Franklin KBJ (2004) Mouse Brain in Stereotaxic Coordinates

Perez SE, He B, Muhammad N, Oh KJ, Fahnestock M, Ikonomovic MD & Mufson EJ (2011) Cholinotrophic basal forebrain system alterations in 3xTg-AD transgenic mice. *Neurobiol. Dis.* **41:** 338–352

Perez SE, Lumayag S, Kovacs B, Mufson EJ & Xu S (2009) Beta-amyloid deposition and functional impairment in the retina of the APPswe/PS1DeltaE9 transgenic mouse model of Alzheimer's disease. *Invest. Ophthalmol. Vis. Sci.* **50:** 793–800

Piaceri I, Nacmias B & Sorbi S (2013) Genetics of familial and sporadic Alzheimer's disease. *Front. Biosci. (Elite Ed).* **5:** 167–77

Pierre M & Nunez J (1983) Multisite phosphorylation of tau proteins from rat brain. *Biochem. Biophys. Res. Commun.* **115:** 212–9

Pike CJ, Burdick D, Walencewicz a J, Glabe CG & Cotman CW (1993) Neurodegeneration induced by beta-amyloid peptides in vitro: the role of peptide assembly state. *J. Neurosci.* **13:** 1676–1687

Reitz C & Mayeux R (2014) Alzheimer disease: Epidemiology, diagnostic criteria, risk factors and biomarkers. *Biochem. Pharmacol.* **88:** 640–651

Rhein V, Baysang G, Rao S, Meier F, Bonert A, Müller-Spahn F & Eckert A (2009a) Amyloid-beta leads to impaired cellular respiration, energy production and mitochondrial electron chain complex activities in human neuroblastoma cells. *Cell. Mol. Neurobiol.* **29:** 1063–1071

Rhein V, Song X, Wiesner A, Ittner LM, Baysang G, Meier F, Ozmen L, Bluethmann H, Dröse S, Brandt U, Savaskan E, Czech C, Götz J & Eckert A (2009b) Amyloid-beta and tau synergistically impair the oxidative phosphorylation system in triple transgenic Alzheimer's disease mice. *Proc. Natl. Acad. Sci. U. S. A.* **106:** 20057–62

Robbins TW & Murphy ER (2006) Behavioural pharmacology: 40+ Years of progress, with a focus on glutamate receptors and cognition. *Trends Pharmacol. Sci.* **27:** 141–148

Roher AE, Lowenson JD, Clarke S, Woods AS, Cotter RJ, Gowing E & Ball MJ (1993) beta-Amyloid-(1-42) is a major component of cerebrovascular amyloid deposits: implications for the pathology of Alzheimer disease. *Proc. Natl. Acad. Sci.* **90:** 10836–10840

Ryan NS & Rossor MN (2010) Correlating familial Alzheimer's disease gene mutations with clinical phenotype. *Biomark. Med.* **4:** 99–112

Saunders AM, Strittmatter WJ, Schmechel D, George-Hyslop PH, Pericak-Vance MA, Joo SH, Rosi BL, Gusella JF, Crapper-MacLachlan DR, Alberts MJ et al. (1994) Association of apolipoprotein E allele epsilon 4 with late-onset sporadic Alzheimer's disease. *Am. J. Med. Genet.* **54:** 286–8

Scheltens P, Blennow K, Breteler MMB, de Strooper B, Frisoni GB, Salloway S & Van der Flier WM aria (2016) Alzheimer's disease. *Lancet (London, England)* **388:** 505–517

Schön C, Hoffmann NA, Ochs SM, Burgold S, Filser S, Steinbach S, Seeliger MW, Arzberger T, Goedert M, Kretzschmar HA, Schmidt B & Herms J (2012) Long-Term In Vivo Imaging of Fibrillar Tau in the Retina of P301S Transgenic Mice. *PLoS One* **7:** 1–9

Selden SC & Pollard TD (1983) Phosphorylation of microtubule-associated proteins regulates their interaction with actin filaments. *J. Biol. Chem.* **258:** 7064–7071

Selkoe DJ (1991) The molecular pathology of Alzheimer's disease. *Neuron* **6:** 487–498

Selkoe DJ (1998) The cell biology of beta-amyloid precursor protein and presenilin in Alzheimer's disease. *Trends Cell Biol* **8:** 447–453

Selkoe DJ & Hardy J (2016) The amyloid hypothesis of Alzheimer's disease at 25 years. *EMBO Mol. Med.* **8:** 595–608

Serrano-Pozo A, Frosch MP, Masliah E & Hyman BT (2011) Neuropathological alterations in Alzheimer disease. *Cold Spring Harb. Perspect. Med.* **1:** 1–23

Seubert P, Vigo-Pelfrey C, Esch F, Lee M, Dovey H, Davis D, Sinha S, Schlossmacher M, Whaley J & Swindlehurst C (1992) Isolation and quantification of soluble Alzheimer's beta-peptide from biological fluids. *Nature* **359:** 325–327

Shah TM, Gupta SM, Chatterjee P, Campbell M & Martins RN (2017) Beta-amyloid sequelae in the eye: a critical review on its diagnostic significance and clinical relevance in Alzheimer's disease. *Mol. Psychiatry***:** 1–11

Sherrington R, Rogaev EI, Liang Y, Rogaeva EA, Levesque G, Ikeda M, Chi H, Lin C, Li G, Holman K, Tsuda T, Mar L, Foncin J-F, Bruni AC, Montesi MP, Sorbi S, Rainero I, Pinessi L, Nee L, Chumakov I, et al (1995) Cloning of a gene bearing missense mutations in early-onset familial Alzheimer's disease. *Nature* **375:** 754–760

Small DH & Cappai R (2006) Alois Alzheimer and Alzheimer's disease: A centennial perspective. *J. Neurochem.* **99:** 708–710

Snyder SW, Ladror US, Wade WS, Wang GT, Barrett LW, Matayoshi ED, Huffaker HJ, Krafft GA & Holzman TF (1994) Amyloid-beta aggregation: selective inhibition of aggregation in mixtures of amyloid with different chain lengths. *Biophys. J.* **67:** 1216–1228

Sofroniew M V. & Vinters H V. (2010) Astrocytes: Biology and pathology. *Acta Neuropathol.* **119:** 7–35

Stelzmann RA, Norman Schnitzlein H & Reed Murtagh F (1995) An english translation of alzheimer's 1907 paper. *Clin. Anat.* **8:** 429–431

Streilein JW (2003) Ocular immune privilege: therapeutic opportunities from an experiment of nature. *Nat. Rev. Immunol.* **3:** 879–89

Takahashi RH (2004) Oligomerization of Alzheimer's -Amyloid within Processes and Synapses of Cultured Neurons and Brain. *J. Neurosci.* **24:** 3592–3599

Thal DR, Rub U, Orantes M & Braak H (2002) Phases of A -deposition in the human brain and its relevance for the development of AD. *Neurology* **58:** 1791–1800

Tseng BP, Green KN, Chan JL, Blurton-Jones M & LaFerla FM (2008) A?? inhibits the proteasome and enhances amyloid and tau accumulation. *Neurobiol. Aging* **29:** 1607–1618

Tzekov R & Mullan M (2014) Vision function abnormalities in Alzheimer disease. *Surv. Ophthalmol.* **59:** 414–433

Verkhratsky A, Marutle A, Rodríguez-Arellano JJ & Nordberg A (2015) Glial Asthenia and Functional Paralysis. *Neurosci.* **21:** 552–568

Weingarten MD, Lockwood AH, Hwo SY & Kirschner MW (1975) A protein factor essential for microtubule assembly. *Proc. Natl. Acad. Sci. U. S. A.* **72:** 1858–62

White KG & Ruske AC (2002) Memory deficits in Alzheimer's disease: The encoding hypothesis and cholinergic function. *Psychon. Bull. Rev.* **9:** 426–437

Whitson JS, Selkoe DJ & Cotman CW (1989) Amyloid beta protein enhances the survival of hippocampal neurons in vitro. *Science (80-.).* **243:** 1488–1490

Williams PA, Thirgood RA, Oliphant H, Frizzati A, Littlewood E, Votruba M, Good MA, Williams J & Morgan JE (2013) Retinal ganglion cell dendritic degeneration in a mouse model of Alzheimer's disease. *Neurobiol Aging* **34:** 1799–1806

Williamson J, Goldman J & Marder KS (2009) Genetic Aspects of Alzheimer Disease. *Neurologist* **15:** 80–86

Wirths O & Bayer TA (2010) Neuron Loss in Transgenic Mouse Models of Alzheimer's Disease. *Int. J. Alzheimers. Dis.* **2010:** 1–6

Yankner B, Duffy L & Kirschner D (1990) Neurotrophic and neurotoxic effects of amyloid beta protein: reversal by tachykinin neuropeptides. *Science (80-.).* **250:** 279–282

Yao J, Irwin RW, Zhao L, Nilsen J, Hamilton RT & Brinton RD (2009) Mitochondrial bioenergetic deficit precedes Alzheimer's pathology in female mouse model of Alzheimer's disease. *Proc. Natl. Acad. Sci.* **106:** 14670–14675

Zahs KR & Ashe KH (2010) 'Too much good news' - are Alzheimer mouse models trying to tell us how to prevent, not cure, Alzheimer's disease? *Trends Neurosci.* **33:** 381–389

Zhang Y & Stone J (1997) Role of astrocytes in the control of developing retinal vessels. *Invest Ophthalmol.Vis.Sci.* **38:** 1653–1666